Plant-derived nanostructures: types and applications

Reza Mohammadinejad,[1] Samaneh Karimi,[2] Siavash Iravani[3,*] and Rajender S. Varma[4,*]

[1]Department of Agricultural Biotechnology, College of Sciences and Modern Technologies, Graduate University of Advanced Technology, Kerman, Iran.

[2]The New Zealand Institute for Plant & Food Research, 7608 Lincoln, New Zealand.

[3]Biotechnology Department, Faculty of Pharmacy and Pharmaceutical Sciences, Isfahan University of Medical Sciences, Isfahan, Iran.

[4]Sustainable Technology Division, National Risk Management Research Laboratory, US Environmental Protection Agency, MS 443, 26 West Martin Luther King Drive, Cincinnati, Ohio, 45268, USA.

***Corresponding Authors:**

Rajender S. Varma, E-mail: Varma.Rajender@epa.gov

Siavash Iravani, E-mail: siavashira@gmail.com

Graphical abstract:

Significant recent developments in plant-derived nanostructures, their classes, and vital applications are discussed with insight into their use as a bio-renewable, sustainable, and diversified resource for the production of useful nanostructures.
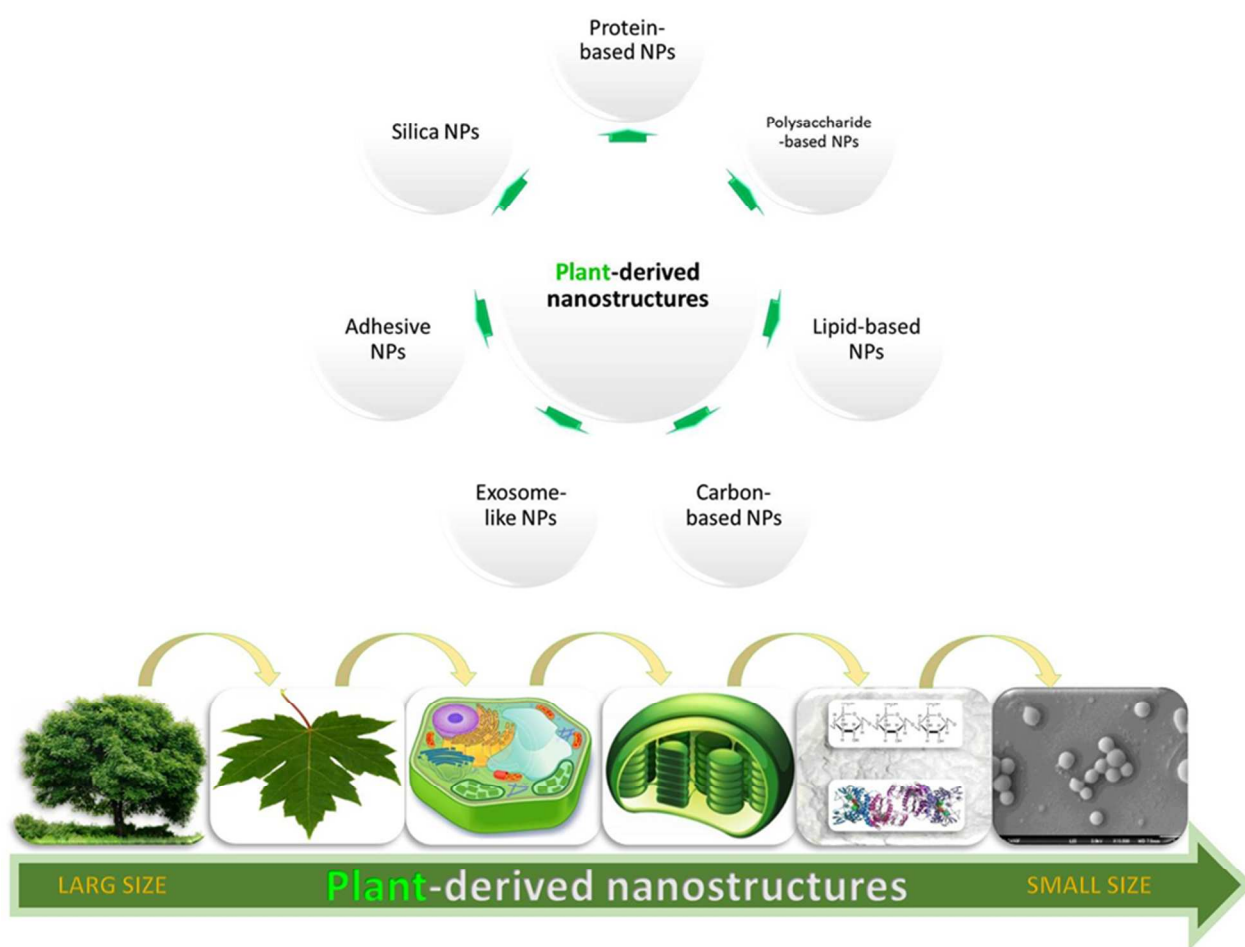
Abstract

Plant-derived nanostructures and nanoparticles (NPs) have functional applications in numerous disciplines such as health care, food and feed, cosmetics, biomedical science, energy science, drug-gene delivery, environmental health, and so on. Consequently, it is imperative for researchers to understand that plants are cost-effective, sustainable and renewable platforms, and therefore, they are ideal sources for production of natural NPs. This critical review discusses significant recent developments pertaining to plant-derived nanostructures, their classes, and vital applications. The aim is to provide insight into the use of plants as a bio-renewable, sustainable, diversified resource and platform for the production of useful nanostructures and NPs, with functions in various fields, including medicine, industry, agriculture, and pharmaceuticals.

Table of content

1. Introduction

Nanostructures and nanoparticles (NPs) have been extensively studied owing to their extremely diminutive size and large surface-to-volume ratio, which contribute to both physical and chemical differences in their properties (*e.g.,* mechanical, biological and sterical properties, catalytic activity, thermal and electrical conductivity, optical absorption, and melting point), when compared to bulk materials of the identical chemical composition. These nanostructures and NPs have been used in areas such as mechanics, optics, biomedical sciences, chemicals, electronics, space industries, drug-gene delivery, energy science, catalysis [1, 2], optoelectronic devices [3, 4], photo-electrochemical applications [5], and nonlinear optical devices [6, 7]. For instance, biocompatible macromolecules such as plant proteins can be used as drug carriers. Azmi *et al.*,[8] reported the use of ultra-sensitive, silicon nanowire-based biosensor devices for the detection of 8-hydroxydeoxyguanosine (8-OHdG), a biomarker for prostate cancer risk. The speed, sensitivity, and ease of biomarker detection using these ultra-sensitive biosensors render them ideal for eventual point-of-care diagnostics. Moreover, a range of nanometer-sized materials, including metal and metal oxide NPs, semiconductor quantum dots, carbon nanomaterials and polymer NPs have been used for various important pharmaceutical and medical applications (for example, nano polymerase chain reaction, nano-PCR). This strategy afforded potentially powerful PCR technology, with unprecedented sensitivity, selectivity, and extension rates [9, 10].

Nanomaterials are generally prepared by a variety of mechanical, physical, and chemical approaches. Organisms (microorganisms and plants) possess unique properties which offer many advantages, including widespread availability, sustainability, and inherent inclusion of chemical

functionality, biocompatibility, and biodegradability [11]. Researchers have found inspiration from viruses, bacteria, fungi, algae, and biomolecules to produce biomimetic nanostructures for various applications. For example, the application of plant virus-derived nanostructures in materials science, biomedical research, and engineering has been recently advanced by the development of fluorescence-labeled viruses for optical imaging in tissue culture and pre-clinical animal models. Most studies have focused their attention on the applications of viruses chemically modified with organic dyes. Shukla *et al*., [12] studied genetically-engineered virus-based biomaterials that incorporated green or red fluorescent proteins, and reported that the genetic introduction of imaging moieties was advantageous because post-harvest modification was not required, thus minimizing the number of manufacturing steps needed and maximizing the yield of each fluorescent probe.

Plants have the ability of producing a variety of highly ordered hierarchical structures, and they can generate such structures effortlessly in various sizes. They present a range of constructions which comprise the natural fractal geometry of branches to form the barbed raphide crystals and thin stacks of grana thylakoids in chloroplasts. Actually, organisms can produce a vast variety of sophisticated inorganic materials. Biomolecules offer unique functionalities such as specific recognition capabilities or catalytic activity. Biological subunits, based on these recognition capabilities, can self-assemble into defined superstructures with unique shapes. Moreover, they respond to multiple physical, chemical, or biological stimuli, and consequently provide a potential means for manufacturing nano-machines [13]. There is typically a high level intricacy in natural plant structures at the micrometer and nanometer scales which is the representation of the sophistication of current engineered materials and systems. There are various synthetic methods to transform highly structured plant materials into functional materials

so as to exploit their intrinsic natural morphology. For instance, it is becoming common to utilize new hybrid structures for drug delivery, environmental remediation, energy generation, or bio-templated nanofabrication. Furthermore, a higher biodegradability trait is generated as a consequence of the direct incorporation of plant structures within polymeric and carbonaceous materials; this bodes a high level of promise for plant composites in biomedical and biosensing applications[14-20]. Plants are capable of generating a wide variety of advanced nanostructures matching the sophistication of current engineered materials, wherein plant biomolecules mediate the safest and most cost-effective large-scale production of biocompatible NPs. Zein, starch, and ivy NPs are just a few examples of biomolecules which have broad important applications in various pharmaceutical and medical fields. This review begins with a description of plant-derived nanostructures and NPs as building blocks for nanotechnology and their important applications. The advantages of using bio-renewable and bio-degradable plants and agricultural residues as sources for nanostructure production are also highlighted (Figure 1). An integral portion of this article focuses on plant-derived NPs and their significance, and a brief discussion on the important role of plants in nanoparticle synthesis is provided. Moreover, the diverse applications of plant-derived nanostructures and NPs in biology, medicine, and pharmacy are discussed in this review.
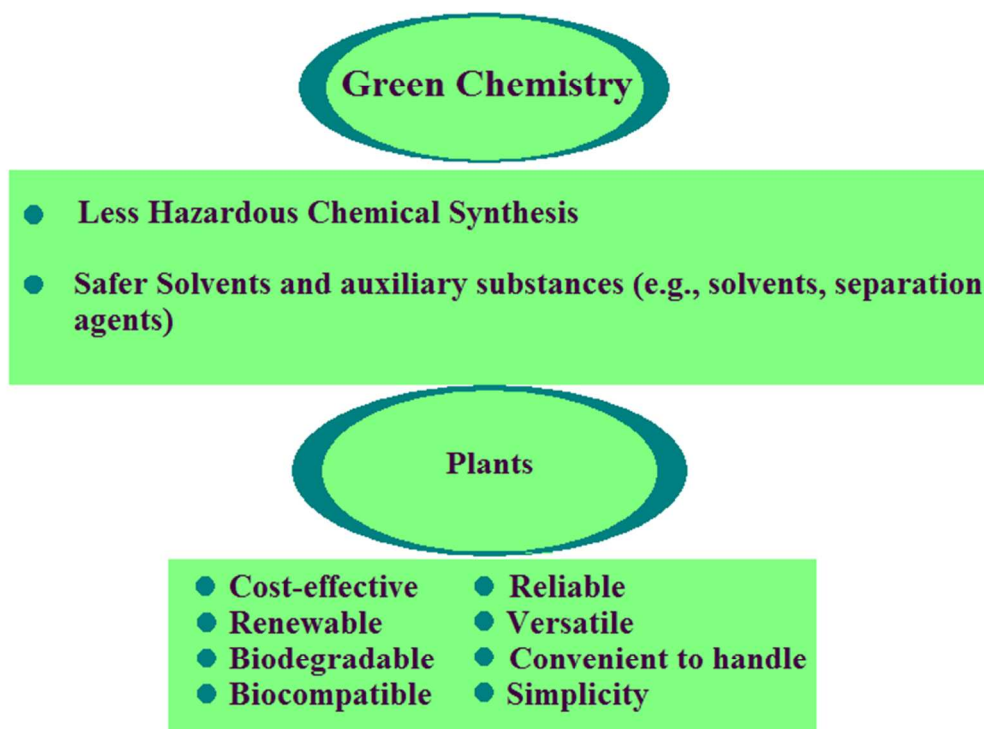
Figure 1. Salient advantages of using plants and agricultural residues as resources for nanostructure production

2. Plants and green nanotechnology

In green nanotechnology, plants have been used owing to their nontoxic chemical constituents and natural materials. Green nanotechnology helps to eliminate or minimize harmful polluting substances in the synthesis of nanomaterials (Figure 2). There are nearly 300,000 plant species in the world which convert sunlight energy into organic chemical energy, in the form of carbohydrates, via photosynthesis [21]. Bioactive and biodegradable compounds obtained from medicinal herbs are very effective for the treatment of several human diseases. For instance, taxol (an approved anticancer drug) and silymarin has been identified as the most effective

therapy for liver diseases. Plants are the source of raw materials, such as wood, resins, oils, and dyes for agro-based industries. Production of biofuels from plants (*e.g.,* sugarcane and jatropha) has become a potential alternative for fossil fuels. Apart from their commercial value, plants are advantageous because they clean the atmosphere, water, and soil via uptake of large amounts of CO_2, heavy metals, and other pollutants. In addition, the significant potential for plant nanostructures has been realized.
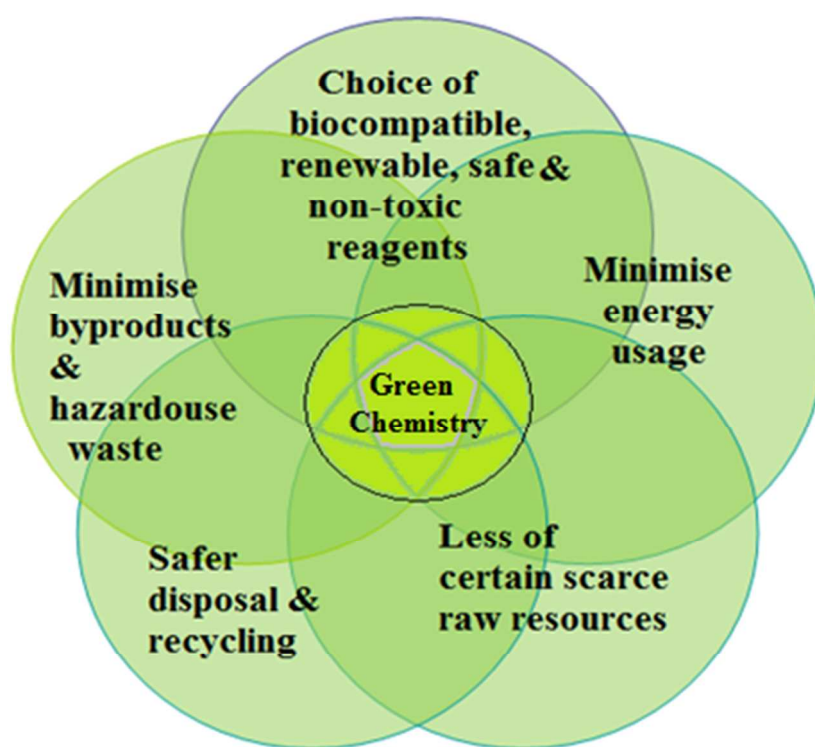
Figure 2. Principles of green chemistry for the production of safer and more sustainable nanomaterials via sustainable nano-manufacturing processes.

2.1. Role of plants and phytochemicals in nanoparticle synthesis

Phytochemicals and plant extracts can be used as reducing and stabilizing agents for synthesis of metal and metal oxide NPs in a single-step green process (Table 1). The only way to develop these "green" processes is to adapt benign synthesis approaches that use mild reaction conditions and non-toxic reaction precursors[22-33]. This biogenic reduction of metal ions to metallic NPs is inexpensive, non-toxic, eco-friendly, expeditious, and readily conducted at ambient temperature and pressure with great potential for scale up. Synthesis mediated by plant extracts is an environmentally friendly option as the reducing agents involved encompass various water-soluble plant metabolites (*e.g.,* alkaloids, phenolic compounds, quinones, organic acids, flavonoids, terpenoids, and catechins), and co-enzymes. Extracts from a diverse range of plant species are efficaciously used for the manufacture of metal and metal oxide NPs. In addition to plant extracts, live plants can also be used for nanoparticle synthesis[34-36]. Green synthesis of metal and metal oxide NPs by plants is mainly advantageous in terms of environmental friendliness. But, major drawbacks associated with this green process are longer reaction times, tedious purification steps, and greater sizes of all NPs and poor understanding of the underlying mechanisms. Optimization of these green chemistry methods is critical for fast and clean synthesis of NPs with desired sizes and morphologies. Plant mediated synthesis of NPs is conferred due to the presence of phytochemicals and biomolecules such as proteins, amino acids, vitamins, polysaccharides, polyphenols, terpenoids, and organic acids. These molecules can be used in synthesis, and also in stabilization of metal and metal oxide NPs formed with desired size

and shape. Studies have indicated that these molecules not only play a role in reducing the ions

to nanosize, but also play an important role in the capping of NPs [20, 23, 34, 37-48].

Table 1. Important examples of plants and phytochemicals in the synthesis of nanoparticles.

Plants	Nanoparticles	Phytochemicals/biomolecules	References
Allium sativum	Au	Proteins	[49]
Aloe barbadensis	CuO	Phenolic compounds, Terpenoids, Proteins	[50]
Alternanthera sessilis Linn.	Ag	Alkaloids, Tannins, Ascorbic acid, Carbohydrates, Proteins	[51]
Andrographis paniculata Nees.	Ag	Hydroxyflavones, Catechins	[52]
Annona squamosa	Pd	Secondary metabolites contained –OH group	[53]
Astragalus gummifer Labill.	Ag	Proteins	[54]
Azadirachta indica	Ag	Reducing sugars, Terpenoids	[55]
Azadirachta indica A. Juss.	Au	Salanin, Nimbin, Azadirone, Azadirachtins	[56]
Benincasa hispida	Au	Polyols	[57]
Calotropis procera L.	Cu	Cysteine protease and tryptophan with functional groups of amines, alcohols, ketones, aldehydes, and carboxylic acids	[58]
Camellia sinensis	Au	Polyphenolic compounds	[59]
Carica papaya (fruit	Ag	Hydroxyflavones,	[60]

extract)		Catechins	
Carica papaya (callus extract)	Ag	Proteins and other ligands	61
Cinnamomum zeylanicum	Pd	Terpenoids (*e.g.,* linalool, methyl chavicol, and eugenol)	62, 63
Cinnamomum camphora	Pd	Polyol components, Water soluble heterocyclic components	64
Citrullus colocynthis	Ag	Polyphenols with aromatic ring and bound amide region	65
Coleus aromaticus Lour.	Ag	Flavonoids, Lignin	66
Corriandrum sativum	ZnO	Phyto-constituents such as alcohol, aldehyde and amine	67
Cycas leaf	Ag	Polyphenols, Glutathiones, Metallothioneins, Ascorbates	68
Cyperus sp.	Ag	Flavones, Quinones, Organic acids	69
Datura metel	Ag	Plastohydroquinone, plastrocohydroquinol	70
Delonix elata	Ag	Phenolic compounds, Flavonoids	42
Desmodium triflorum	Ag	H^+ ions produced a long with NAD during glycolysis, Water-soluble antioxidative agents like ascorbic acids	71
Diopyros kaki	Pt	Terpenoids, Reducing sugars	72
Dioscorea bulbifera	Ag	Polyphenols, Flavonoids	73
Dioscorea oppositifolia	Ag	Polyphenols with aromatic	74

13

		ring and bound amide region	
Eclipta prostrata	TiO$_2$	Heterocyclic compounds such as flavones	75
Elettaria cardamomom	Ag	Alcohols, Carboxylic acids, Ethers, Esters, Aliphatic amines	76
Eucalyptus hybrida	Ag	Flavanoid and terpenoid constituents	77
Euphorbia nivulia	Cu	Peptides, Terpenoids	78
Festuca rubra	Ag	Reducing sugars, Antioxidant compounds, Ascorbic acid	79
Gardenia jasminoides Ellis.	Pd	Geniposide, Chlorogenic acid, Crocins, Crocetin	80
Glycine max	Pd	Proteins, Amino acids	81
Glycyrrhiza Glabra	Ag	Flavonoids, Terpenoids, Thiamine	82
Hibiscus cannabinus	Ag	Ascorbic acid	83
Hydrilla sp.	Ag	Flavones, Quinones, and organic acids (*e.g.,* oxalic, malic, tartaric, and protocatecheuic acid)	69
Hydrilla verticilata	Ag	Proteins	84
Justicia gendarussa	Au	Polyphenol, Flavonoid compounds	85
Lantana camara	Ag	Carbohydrates, Glycosides, Flavonoids	86
Leonuri herba	Ag	Polyphenols, Hydroxyl groups	87

14

Magnolia kobus	Au	Proteins and metabolites (e.g., terpenoids having functional groups of amines, aldehydes, carboxylic acid, and alcohols)	88
Mentha piperita	Au & Ag	Menthol	89
Mirabilis jalapa	Au	Polyols	90
Morinda pubescens	Ag	Hydroxyflavones, Catechins	91
Ocimum sanctum	Ag & Pt	Phenolic and Flavanoid compounds, Proteins, Ascorbic acid, Gallic acid, Terpenoids, Proteins and amino acids	92, 93
Ocimum tenuiflorum	Ag	Polysaccharides	94
Parthenium hysterophorus	Ag	Hydroxyflavones, Catechins	95
Pedilanthus tithymaloides	Ag	Proteins, Enzymes	96
Pelargonium graveolens	Ag	Proteins, Terpenoids and other bio-organic compounds	97
Phoma glomerata	Ag	Proteins, Amino acids	38
Pinus eldarica	Ag	polyphenolic compounds	24
Pinus resinosa	Pt	Lignin	98
Piper betle	Ag	Proteins	99
Piper betle	Pd	Flavonoids, Terpenoids, Proteins	100
Piper nigrum	Ag	Proteins	101

15

Plumeria rubra	Ag	Proteins	102
Saraca indica	Au	Polyphenolic compounds	103
Sesuvium portulacastrum	Ag	Proteins, Flavones, Terpenoids	104
Solanum lycopersicums	Au & Ag	Flavonoids, Alkaloids, Antioxidant vitamins, Carotenoids (lycopene), Polyphenols	105
Solanum xanthocarpum	Ag	Phenolics, Alkaloids, Sugars	106
Sorghum bicolor Moench	Ag & Fe	Polyphenols	107
Syzygium aromaticum	Au	Flavonoids	108
Terminalia arjuna	Cu	Flavonones, Terpenoids	109
Terminalia catappa	Au	Hydrolysable tannins	110
Terminalia chebula	Ag	Polyphenols present in the form of hydrolysable tannins	111
Trianthema decandra	Ag	Hydroxyflavones, Catechins	112
Tridax procumbens	CuO	Water-soluble carbohydrates	113
Zingiber officinale	Au & Ag	Alkanoids, Flavonoids	114

2.2. Nano-agriculture: nanobiotechnology applications to crop-science

Nano-pesticides or plant protection products in nano formulation represent an emerging technological development that, in relation to pesticide use, could offer a range of benefits such as increased efficacy, durability, and a reduction in the amounts of required active ingredients [115]. Nanofertilizers are able to synchronize the release of nutrients with their plant uptake, thus avoiding the loss of nutrients and reducing the risks of groundwater pollution [116]. Biochar, a carbon-rich product, has been shown to suppress plant disease and improve agriculture [117]. Moreover, NPs are able to deliver DNA and chemicals into plant cells [118]. While carbon nanotubes (CNTs) have been shown to dramatically improve germination of some comestible plants, deficiencies in behavior consistency and reproducibility have arisen, in part, due to the variability of the CNTs used; they have shown promise as regulators of seed germination and plant growth. Khodakovskaya *et al.*, [119] demonstrated that multi-walled CNTs (MWCNTs) enhanced the growth of tobacco cell culture (55-64% increase over control) over a wide range of concentrations (5-500 μg/mL). Interestingly, they found a correlation between the activation of growth in cells exposed to MWCNTs and the up-regulation of genes involved in cell division/cell wall formation and water transport. The expression of the tobacco aquaporin gene (*NtPIP1*) and the production of the NtPIP1 protein were significantly increased in cells exposed to MWCNTs in comparison to control cells. The expression of marker genes for cell division (*CycB*) and cell wall extension (*NtLRX1*) was also up-regulated in cells exposed to MWCNTs, compared to control cells. Moreover, Giraldo *et al.*, [120] showed that single-walled CNTs get passively transported and irreversibly localized within the lipid envelope of extracted plant

chloroplasts, thus promoting over three times higher photosynthetic activity than that of controls, and enhancing maximum electron transport rates. The single-walled CNTs -chloroplast assemblies also enabled higher rates of leaf electron transport *in vivo* through a mechanism consistent with augmented photo-absorption. Concentrations of reactive oxygen species (ROS) inside extracted chloroplasts were significantly suppressed by delivering poly(acrylic acid)-nanoceria or single-walled CNTs -nanoceria complexes. Furthermore, single-walled CNTs enabled near-infrared fluorescence monitoring of nitric oxide both *ex vivo* and *in vivo*, thus illustrating that a plant can be augmented to function as a photonic chemical sensor[53].

Nano-bionic engineering of plant functions may contribute to the development of biomimetic materials for light-harvesting and biochemical detection with regenerative properties and enhanced efficiency. Chandra *et al*., [121] developed biocompatible amine-functionalized fluorescent carbon dots and isolated them for gram-scale applications. These carbogenic quantum dots can strongly conjugate over the surface of the chloroplast, and due to this strong interaction, the former can easily transfer electrons to the latter by assistance from absorbed light or photons. An exceptionally high electron transfer from carbon dots to the chloroplast can directly affect the whole chain electron transfer pathway in a light-assisted reaction of photosynthesis, where electron carriers play an important role in modulating the system. As a result, carbon dots can promote photosynthesis by modulating the electron transfer process, as they are capable of hastening the conversion of light energy to electrical energy, and finally, to chemical energy, as assimilatory power (ATP and NADPH).

3. Plant-derived nanostructures: types, preparation and applications

Plants have numerous benefits as natural nano-factories. For instance, gliadin NPs have been used as carriers for the oral administration of lipophilic or anticancer drugs. Yi *et al*., [122] developed an infusion-dialysis procedure for isolating spherical tea NPs from green tea with diameters of 100-300 nm and zeta potential of −26.52 mV at pH 7, and explored the potential of these NPs as multifunctional nanocarriers for cancer therapy *in vitro*. Daus and Heinze prepared spherical xylan NPs with mean diameters ranging from 162 to 472 nm for drug delivery applications [123]. Kung *et al*., [124] used an essential oil from peppermint plants to prepare luminescent NPs; such peppermint oil-derived NPs had a narrow particle size distribution (approximately 1.5 ± 0.5 nm) with prominent blue emission under ultraviolet irradiation. In addition, Johnson-Buck *et al*., [125] reported the synthesis of nanocrystals from indigo dye by re-precipitation, by using the plant *Indigofera tinctoria* as a natural source of indigo dye. In one study, Koga *et al*., [126] demonstrated the fabrication of highly transparent conductive networks on cellulose nanopaper. Cellulose nanofibers with width of approximately 15 nm and length of more than several mm were extracted from softwood chips (Sitka spruce, *Picea sitchensis*). The cellulose nanopaper, acted as both filter and transparent flexible substrate for the silver nanowires and CNTs breaking new ground in the creation of next-generation paper electronics. Gilca *et al*., presented a physical method to obtain NPs based on lignin by acoustic irradiation [127]. Athinarayanan *et al*. [128] synthesized spherical biogenic silica NPs (~10-30 nm) from acid pretreated rice husks via calcination. Photoluminescence studies indicated that amorphous silica was an appropriate resource of silicon NPs for solar cell or biomedical applications. In another

study, Mehta *et al.*, [129] reported a one-pot method for the green synthesis of water-dispersible

fluorescent carbon dots (~3 nm size) using *Saccharum officinarum* juice; they served as excellent

fluorescent probes for cellular imaging of bacteria (for example, *Escherichia coli*) and yeast

(*Saccharomyces cerevisiae*). Yuan *et al.*, [130] demonstrated an efficient and low-cost pathway to

nitrogen-doped carbon dots by using widely available plant cytoplasm as both the carbon and

nitrogen sources; they served as label-free and highly sensitive and selective probes for detecting

p-nitroaniline in both soils and aqueous media. Reddy *et al.,*[131] prepared wheat glutenin NPs

(~70-140 nm) for drug delivery applications. Strong acidic or alkaline conditions provided

glutenin NPs with low diameters and the particles were more stable under pH 7 rather than pH of

4. [131] Ng *et al.,*[132] synthesized equilateral hexagonal EMT-type zeolite NPs from rice husk..

The following section aims to provide insight into the use of plants as a bio-renewable,

sustainable, diverse source and platform for the production of useful nanostructures and NPs,

with applications in various disciplines, including medicine, industry, and agriculture (Table 2).

Table 2. Some important applications of plant-derived nanostructures.

Plant-derived nanostructures	*Applications*	*References*
Proteins-based NPs	- Controlled drug & gene delivery - Bioactive compound delivery -Tissue engineering -Food industry -Improvement of oral bioavailability of drugs - Drug loaded carriers for medical applications (*e.g.,* gliadin)	133, 69, 70, 134
Polysaccharides-based NPs	-Drug delivery systems based on nanocellulose -Drug excipients - Blood vessel replacement -Soft-tissue-ligament, meniscus & cartilage	135, 136, 137

	replacements	
	- Nucleus pulposus replacement	
	-Tissue repair, regeneration & healing	
Carbon-based nanostructures	-Bioimaging	[138, 139, 140, 141]
	-Biosensor	
	-Optoelectronic	
	-Photocatalyst	
	- Electrodes in energy storage devices	
	-Organic photovoltaic cells	
	- Fluorescent ion detection	
Exosome-like NPs	-Oral delivery	[142, 143]
	-Modulation of intestinal tissue renewal processes	
	- Regulation of gene expression	
Adhesive NPs	-Tissue engineering & biomedical applications	[144, 145]
	- Platelet aggregation, leading to clotting, & the sealing of wounds	
	-Cosmetics	
Silica NPs	- Lithium-ion battery	[146, 147]
	-Nanoelectronics	
	-Photonics	
	- Food additive	
	-Energy harvesting	
	-Energy storage	
	-Drug carriers	
	-Tissue engineering	
	-Anti-caking agent in the food industry	
Lipids-based NPs	-Generation of soft nanomaterials such as nanotubes, nanofibers, gels and surfactants	[148, 149]
	-Biomedical applications	

21

3.1. Protein-based NPs

Protein bio-macromolecules, comprising a family of *L*-α-amino acids with different characteristics, perform many functions within living organisms. Proteins consisting four distinct structures can be folded into three-dimensional (3D) structures, the primary structure being the amino acid sequence. The secondary structure consists of regularly repeating local structures stabilized by hydrogen bonds, and the most common examples are the alpha-helix, beta-sheet, and turns. The tertiary structure includes the overall form of a single protein molecule; the spatial relationship of the secondary structures to one another. The tertiary structure not only is generally stabilized by non-local interactions, most commonly via the formation of a hydrophobic core, but also through salt bridges, hydrogen bonds, disulfide bonds, and post-translational modifications. The quaternary structure, usually called protein subunits in this context, is the structure formed by several protein molecules (polypeptide chains), which acts as a single protein complex. Most of proteins are enzymes involved in metabolism. Furthermore, there are proteins, such as actin and myosin in muscle which are responsible for cell structural properties. Additionally, some proteins are important in cell signaling, immune response, cell adhesion, and importantly, there are proteins essential for an animals' diet [133].

3.1.1. Grain protein NPs

Corn, wheat, and soybeans also containing proteins and are generally referred as readily available plant proteins or cereal proteins which are biodegradable, and are considerably less allergic in contrast to animal proteins, such as bovine collagen (Figure 3). Plant proteins are generated as co-products when cereal grains are processed for food or fuel, and have limited non-

food applications. The major plant proteins include zein in corn, soy proteins, and wheat proteins (gluten, gliadin, and glutenin), in addition to wheat gluten, peanuts, sorghum, millets, and other cereal grains. Widely available plant proteins have lower molecular weights than collagen or silk and they possess higher net negative charges than collagen and silk, and consequently would be more suitable for the delivery of positively charged drugs. Plant proteins, similarly, have polar hydrophilic amino acids that renders them more favorable to attract cells. The wide range of isoelectric points for plant proteins allows researchers to choose appropriate proteins for delivering specific drugs into the body [150, 151].
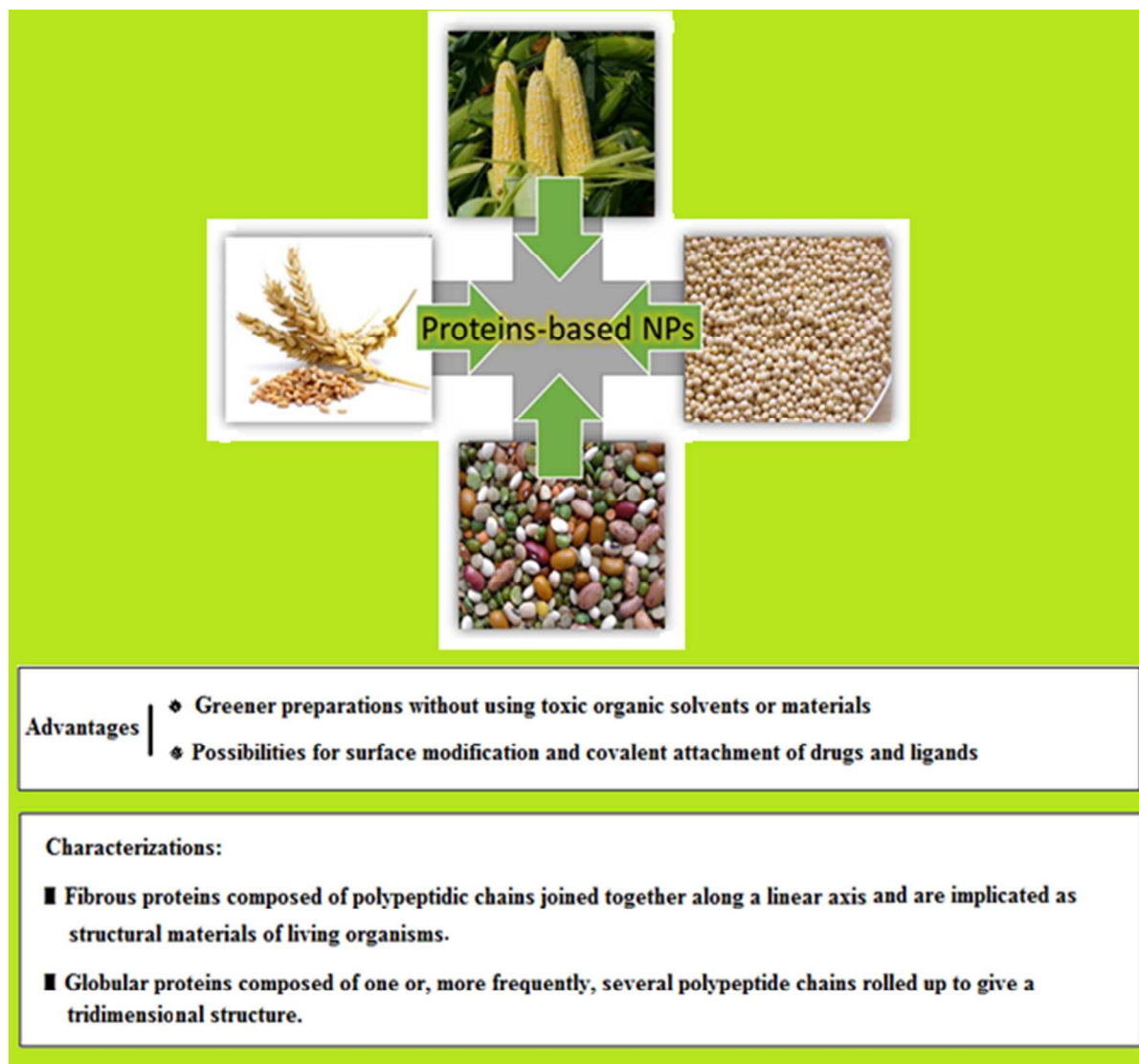
Figure 3. Sources of plant proteins, their advantages and characterizations

Zein NPs

Zein is a water-insoluble plant storage prolamine protein from corn (*Zea mays L.*) that has been used extensively in industrial and food applications such as coatings of paper cups, clothing fabrics, adhesives, and binders. [152] Upon cast drying, the acidic treated zein formed films with holes (Figure 4 A and B), while zein treated under the near neutral and basic conditions, formed uniform particles ranging from 100 to 400 nm (Figure 4C–E). Zein has three

quarters of lipophilic and one quarter of hydrophilic amino acid residues, and consists of three

fractions that vary in molecular weight (MW) and solubility namely α-zein (MW, 19-24 kDa; 75-

80% of total protein), β-zein (17-18 kDa, 10-15%), and γ-zein (27 kDa, 5-10%). A large

proportion (>50%) of non-polar amino acids (leucine, proline, alanine, and phenylalanine) in

zein makes it water insoluble. Zein being deficient in essential amino acids, such as tryptophan

and lysine, and hence, is poor in nutritional quality. Commercial zein available in two grades,

yellow and white zein, and its particulate systems have been prepared using phase separation

based on the differential solubility of zein in ethanol and aqueous solution. Zein is approved by

the Food and Drug Administration (FDA) as a generally recognized as safe excipient for

pharmaceutical film coatings. Xu *et al.*, [134] developed biodegradable hollow zein to remove

reactive dyes from simulated post-dyeing wastewater with remarkably high efficiency. Hollow

zein NPs (ZN) have higher adsorption for Reactive Blue 19 than solid structures, and the

adsorption amount has been shown to increase with decrease in temperature and pH or increase

in initial dye concentration. The adsorption capacity of hollow zein has also been shown to be

much higher than that of various biodegradable adsorbents developed to remove reactive dyes.
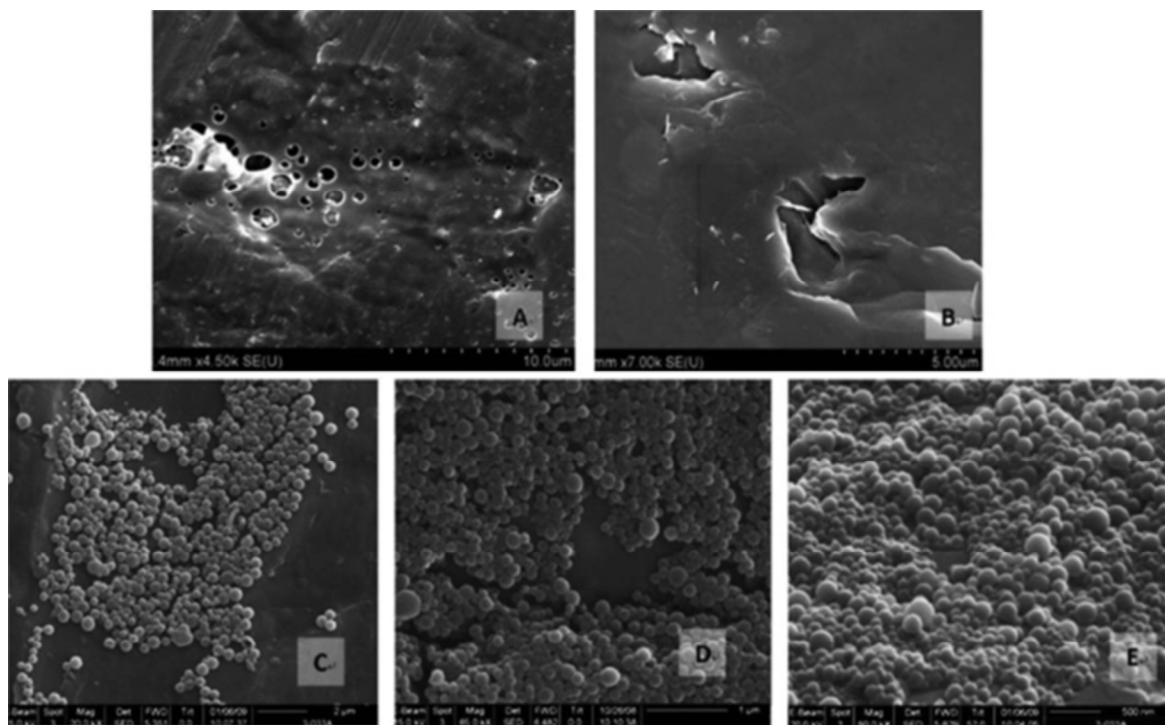
Figure 4. SEM images of pH-treated dried zein samples: (A) Z2.7; (B) Z3.3; (C) Z6.5; (D) Z10.5; and (E) Z12.5 Reproduced with permission from ref [153].

Zein has been used in controlled drug delivery and tissue engineering (Figure 5), as exemplified by zein nanofibers-based siRNA delivery system. Wherein, the amphiphilic property of zein and the size advantage of nanofibers have been brought together; morphological analysis of the GAPDH-siRNA loaded zein nanofibers revealed the proper encapsulation of the siRNA in the polymeric matrix, the loading efficiency of this delivery system being 58.57 ± 2.4 % (w/w). The agarose gel analysis revealed that the zein nanofibers preserved the integrity of siRNA for a longer period even at the room temperature. The *in vitro* release studies not only depicted the sustaining potential of the zein nanofibers but also ensured the release of sufficient quantity of siRNA required to induce the gene silencing effect. The amphiphilic property of zein supported the cell attachment and thereby facilitated the transfection of siRNA into the cells; qRT-PCR

analysis confirmed desired gene silencing effect [154]. In addition, this biodegradable and biocompatible protein can be used for several industrial applications including agriculture, cosmetics, packaging, and pharmaceuticals. For example, controlled delivery of hollow NPs from zein to different organs of mice was achieved via crosslinking using starch-derived non-toxic polycarboxylic acid, citric acid. The NPs showed improved stability in aqueous environment at pH 7.4 without affecting the adsorption of 5-Fluro uracil (5-FU), a common anticancer drug rendering them as potential vehicles for controllable delivery of anticancer therapeutics[155].

Preparation methods	Types of nanostructures	Applications
Liquid–liquid dispersion	Nanoparticles	Drug delivery
Phase separation	Nano-composites	Gene delivery
electrospinning	Hollow nanosphere	Food industry
	Nanofiber	Tissue engineering
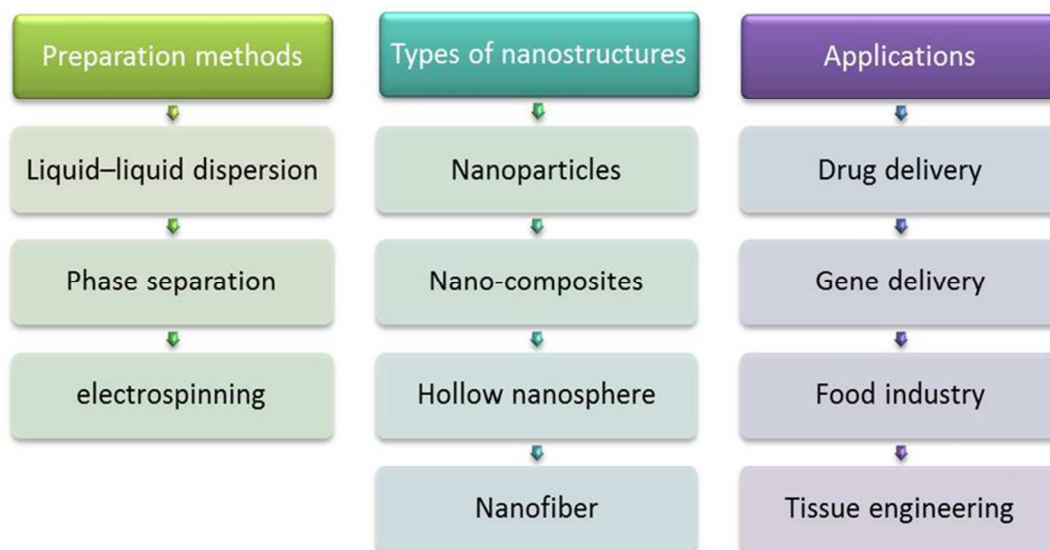
Figure 5. Zein: some important preparations methods, types of nanostructures, and important applications.

In an effort to improve the oral bioavailability of daidzin, an isoflavone glycoside with estrogenic activities, Zou *et al*., [156] designed TPGS 1000 (TPGS) emulsified zein NPs (TZN). ZN

and TZN were fabricated as approximately 200 nm spherical NPs with low polydispersity using an anti-solvent method; the zeta potentials being ~ +25 mV at pH 5.5 and −23 mV at pH 7.4. The addition of TPGS, as an emulsifier, increased the encapsulation efficiency of daidzin in the ZN and daidzin-loaded TZN exhibited a slower daidzin release when compared with the daidzin-loaded ZN, in both simulated digestive fluids and at pH 7.4 buffer. Confocal laser scanning microscopy suggested that the cellular uptake of coumarin-6-labeled TZN in human intestinal epithelial Caco-2 cells is significantly higher than fluorescent ZN. Cellular uptake and transport studies revealed that daidzin in TZN was taken up more efficiently into Caco-2 cells and transported more quickly through a Caco-2 monolayer than through a daidzin solution. A pharmacokinetic study demonstrated that the C_{max} of daidzin in mice, after oral administration of daidzin-loaded TZN, was 5.66 ± 0.16 μM, which was a marked 2.64-fold improvement compared to that of daidzin solution (2.14 ± 0.04 μM).

Xu et al., [134] developed hollow ZN for potential drug delivery applications, with average diameters as small as 65 nm, which were capable of loading a large amount of drug with ability to penetrate into the cell cytoplasm; hollow ZN was capable of loading as much as 369 mg g^{-1} of the drug metformin at an equilibrium concentration of 3 g L^{-1}. Metformin in hollow ZN showed a more sustained and controlled release profile than that in solid ZN; hollow ZN entered fibroblast cells 1 h after incubation. Moreover, Lai et al., [157] proposed a new ZN-encapsulated 5-FU that targets the liver via intravenous delivery. The drug loading was optimized and the in vivo targeting efficiency was increased 31%.

Aswathy et al., [158] reported the synthesis of 5-FU-loaded biocompatible fluorescent ZN. ZN of approximately 800 nm in size that was conjugated with quantum dots (ZnS: Mn). NPs

28

were, in turn, encapsulated with the drug 5-FU, and they were successfully employed for cellular imaging. Biocompatibility studies showed that NPs at higher concentrations were compatible with cells, and were therefore, expected to be promising agents for targeted drug delivery. In another study, Zhang *et al*., [159] prepared and characterized thymol-loaded ZN stabilized with sodium caseinate and chitosan hydrochloride; encapsulated thymol was more effective in suppressing gram-positive bacterium than un-encapsulated thymol for a longer period. Lee *et al*., [160] introduced a novel drug delivery system composed of zein, and demonstrated that ZN protected therapeutic proteins, catalase and SOD, from the harsh conditions found in the gastrointestinal (GI) tract; folate-conjugated catalase or SOD in ZN was able to target activated macrophages, and scavenge ROS generated by macrophages in vitro. Chen *et al*., [161] produced tangeretin-loaded protein NPs by mixing an organic phase containing zein and tangeretin, with an aqueous phase containing β-lactoglobulin. Overall, they demonstrated that protein-based NPs could be used to encapsulate bioactive tangeretin; so that it could be readily dispersed in compatible food products.

Luo *et al*., [162] encapsulated a hydrophobic nutrient, α-tocopherol (TOC), into a zein/chitosan complex wherein physicochemical and structural analysis showed that electrostatic interactions and hydrogen bonds were the major forces responsible for the complex formation. Compared with ZN, the zein/chitosan complex provided better protection of TOC release against GI conditions, due to the chitosan coatings. Luo *et al*., [163] prepared ZN coated with carboxymethyl chitosan (CMCS) to encapsulate vitamin D3 (VD3) and found that VD3 was first encapsulated into ZN using a low-energy phase separation method, and was simultaneously coated with CMCS. Then, calcium was added to cross-link the CMCS to obtain a thicker and denser coating; NPs with CMCS coatings had a spherical structure, with particle size ranging

from 86 to 200 nm. The encapsulation efficiency was greatly improved to 88 % after CMCS coating, compared with 52.2% for those using zein as a single encapsulant. NPs with coatings provided better controlled release of VD3 in both phosphate buffered saline (PBS) medium and simulated GI tract conditions. Photo-stability against UV light was significantly improved as well after encapsulation.

Indole-3-carbinol (I3C) and 3,3′-diindolylmethane (DIM) are two bioactive compounds that are obtained from cruciferous vegetables. However, the stability of these compounds has been a major limitation for their pharmaceutical applications. Luo *et al.*, [164] prepared zein and zein/CMCS NPs to encapsulate I3C and DIM with a combined liquid-liquid phase separation and ionic gelation method; zeta potential decreased from approximately −10 to −20 mV, and the encapsulation efficiency was greatly improved thus both NP formulations providing controlled release of I3C and DIM in PBS. Wu *et al.*, [165] encapsulated two essential oils (EOs), thymol and carvacrol, in zein NPs using a liquid-liquid dispersion method. Reduction of *Escherichia coli* from 0.8 to 1.8 log CFU/mL was achieved in the presence of NPs encapsulating EOs.

Regier *et al.*, [166] fabricated zein nanospheres encapsulating DNA using a coacervation technique, without the use of hazardous solvents or harsh temperatures, resulting in the preservation of DNA integrity and particles with diameters that ranged from 157.8 ± 3.9 nm to 396.8 ± 16.1 nm, depending on the zein to DNA ratio. The spheres protected encapsulated DNA from DNase I degradation, and exhibited sustained plasmid release for at least 7 days, with minimal burst during the initial release phase thus demonstrating robust biocompatibility, cellular association, and internalization.

Gomez-Estaca *et al*., [167] prepared ZN with a compact spherical structure and a narrow size distribution by electro-hydrodynamic atomization, and showed that ZN could be obtained from zein at concentrations ranging from 2.5% to 15% (w/w). The sizes of these particles, ranging from 175 to 900 nm, increased with increasing polymer concentrations. The morphology of the NPs did not change after incorporating curcumin in proportions ranging from 1:500 to 1:10 (curcumin:zein), and the encapsulation efficiency was approximately 85-90%. Fluorescence microscopy images showed that the ensuing nanostructures were similar in form to the matrix systems, with the curcumin homogeneously distributed in the zein matrix. The curcumin remained in an amorphous state in the NPs, as revealed by X-ray diffractometry, which showed close contact with the polymer. After extended storage of three months at 23 °C and 43% relative humidity in the dark, neither the size nor the morphology of the NPs had undergone significant changes, and the curcumin content was not affected. Due to the encapsulation, the curcumin was well dispersed when evaluated in an aqueous food matrix of semi-skim milk.

Jiang *et al*., [168] investigated core-sheath nanofibers prepared using coaxial electro-spinning for providing biphasic drug release profiles. Using ketoprofen (KET) as the model drug, and polyvinylpyrrolidone (PVP) and zein as the sheath polymer and core matrix, respectively, the coaxial process could be carried out smoothly and continuously without any clogging of the spinneret. In this study, SEM and transmission electron microscopy (TEM) demonstrated that the nanofibers were linear with a homogeneous structure, and had a clear core-sheath structure with an average diameter of 730 ± 190 nm, in which the sheath had a thickness of approximately 90 nm. Differential scanning calorimetric (DSC) and X-ray diffraction (XRD) analyses verified that all the components in the core-sheath nanofibers were present in an amorphous state. Attenuated total reflectance Fourier transform infrared spectra (FTIR) demonstrated that both the sheath and

core matrix had good compatibility with KET due to hydrogen bonding. *In vitro* dissolution tests showed that the nanofibers provided an immediate release of 42.3% of the contained KET, follow by a sustained release of the remaining drug over 10 h.

Huang *et al.*, [169] investigated the preparation of drug-loaded fibers using a modified coaxial electro-spinning process, in which only unspinnable solvent was used as the sheath fluid. With a zein/ibuprofen (IBU) co-dissolving solution and *N,N*-dimethylformamide as the core and sheath fluids, respectively, the drug-loaded zein fibers were continuously and smoothly generated without any clogging of the spinneret. Field-emission SEM and TEM observations demonstrated that the fibers had a ribbon-like morphology with a smooth surface. The average fiber diameters were 0.94 ± 0.34 and 0.67 ± 0.21 μm, when the sheath-to-core flow rate ratios were 0.11 and 0.25, respectively. X-ray diffraction and differential scanning calorimetry analyses verified that the IBU was amorphous in all of the fiber composites. FTIR spectra showed that the zein exhibited good compatibility with IBU due to hydrogen bonding. *In vitro* dissolution tests showed that all the fibers provided sustained drug release files via a typical Fickian diffusion mechanism. This modified coaxial electrospinning process could expand the capability for electro-spinning to generate fibers and provide a new method for developing novel drug delivery systems.

Sun *et al.*, [170] evaluated supercritical CO_2 anti-solvent technology for preparing ZN loaded with resveratrol wherein it was found that the resveratrol yield was lower when CO_2 pressure increased, while the loading yield was higher with increased temperature and ratio. The structure of resveratrol-loaded ZN was a matrix with a well-distributed spherical shape and in vitro drug release studies showed that the products exhibited a slower release than resveratrol by

itself. Hu *et al.*, [171] applied solution-enhanced dispersion by supercritical fluids (SEDS) for the production of lutein/ZN and found that NPs with high drug loading and high entrapment efficiency could be prepared using this process. Temperature, pressure, ratio of lutein: zein, and solution flow rate influenced the morphology, drug loading, entrapment efficiency, and mean particle size of the lutein/zein NPs. Lower temperature and solution flow rate, coupled with high pressure, favored smaller and more regular-shaped spheres. The initial burst release was hardly observed in NPs processed at 45°C/10 MPa. Furthermore, the lutein release profile displayed a near zero-order release, which implied that the NPs played a role in controlled lutein release.

Zou *et al.*, [172] fabricated cranberry procyanidins (CPs)-ZN using a modified liquid-liquid dispersion method. They found that the particle size of the CPs-ZN increased from 392 nm to 447 nm, with increasing CPs-to-zein mass ratios from 1:8 to 1:2. The oligomers with higher degrees of polymerization (DP) showed higher loading efficiency than the oligomers with lower DPs, suggesting a greater binding affinity on zein proteins. FTIR spectroscopy suggested that the primary interactions between the CPs and zein were hydrogen bonds and hydrophobic interactions. Cell culture studies using human promyelocytic leukemia HL-60 cells showed that the CPs encapsulated in the NPs had decreased cytotoxicity compared to the CPs.

Zhong *et al.*, [173] used spray-drying to encapsulate a model antimicrobial of lysozyme in corn zein. The effects of the zein/lysozyme (20:1 to 4:1) and zein/thymol (1:0 to 4:1) ratios on the microstructures of the microcapsules, and the *in vitro* release profiles of the encapsulated lysozyme, were investigated; less lysozyme was released at higher pH, resulting from stronger molecular attraction between zein and lysozyme. Nanoscale microcapsule matrix structures were correlated with release characteristics of the encapsulated lysozyme. At intermediate

zein/lysozyme (10:1) and zein/thymol (50:1) ratios, microcapsules had a continuous matrix structure, and revealed sustained release (11-65 %) of lysozyme at pH 6 over 49 days. The nano-scale diameters, biocompatibility, potential for loading a large quantity of drugs, and the ability to penetrate into cells render ZN ideal candidates for transporting various molecules for intracellular drug delivery and tissue engineering for biomedical applications [134].

Gliadin NPs

Ezpeleta *et al*., [174] have studied the feasibility of preparing small-sized carriers from vegetal macromolecules. For this purpose, they selected gliadin (a vegetal protein fraction from wheat gluten) NPs as drug carriers for all-trans-retinoic acid (RA). Their systems were prepared by a desolvation method for macromolecules, which produced gliadin NPs of about 500 nm, with a yield close to 90% of the initial protein in environmentally acceptable solvents such as water and ethanol. Moreover, due to the low solubility of this protein in water and its high hydrophobicity, the gliadin NPs did not require any further chemical or physical treatment for hardening. Gliadin NPs were quite stable over 4 days in PBS, but rapidly degraded over 3 h when incubated in PBS solution containing trypsin. However, chemical cross-linkage of NPs with glutaraldehyde markedly increased their stability. Finally, the *in vitro* release profiles of RA-loaded gliadin NPs showed a biphasic pattern, where an initial burst effect (in which ~ 20% RA was released), followed by zero-order diffusion (release rate 0.065 mg RA/h) was observed. Arangoa *et al*., [175] reported that gliadin NPs dramatically increased carbazole oral bioavailability up to 49%, and provided sustained release properties pertaining to a decrease of the carbazole plasma elimination rate.

α-Tocopherol or vitamin E is widely used as a strong antioxidant in many medical and cosmetic applications. However, it is rapidly degraded in view of its light, heat, and oxygen sensitivity. Thus, all vitamin E formulations must avoid contact with light, heat, and air. Drug-loaded vitamin E carriers are an attractive option, particularly if they are made of bioacceptable macromolecules, such as vegetal proteins. For instance, gliadins, generate NPs by a desolvation method, and may interact with epidermal keratin for therapeutic or cosmetic formulations. vitamin E-loaded gliadin NPs have been characterized based on their size, zeta potential, vitamin E payload, and entrapment efficiency, and it was shown that the gliadin particle size is ~900 nm after vitamin E loading, and their charge is close to zero; these gliadin particles are suitable vitamin E drug carriers, with an optimum encapsulation rate of ~100 vitamin E µg/ gliadin mg, with an efficiency of more than 77%. The release behavior of vitamin E -loaded NPs has been interpreted as a "burst effect," followed by a diffusion process through a homogeneous sphere [176].

Kajal and Misra [177] prepared NPs incorporating tetanus toxoid and a model antigen ovalbumin, and investigated them as delivery vehicles for oral immunization. Gliadin was again used as the carrier because of its biocompatibility, oral bioavailability, and mucoadhesive properties. The size of NPs with ~50% w/w of antigen remained stable over 3 weeks of testing. Chen *et al.*, [178] used an electro-spray deposition system to synthesize gliadin and gliadin-gelatin composite NPs for delivery and controlled release of an anticancer drug (*e.g.,* cyclophosphamide; cyclophosphamide was gradually released from the gliadin NPs for 48 h.

3.1.2. Legume protein NPs

Legumes (Fabaceae or Leguminosae) are the third largest family of flowering plants and the second most important plant family in agriculture. They are particularly interesting because most have the capacity to fix atmospheric nitrogen through mutualistic interactions with rhizobial soil bacteria, a trait that is both ecologically and agriculturally important. The most cultivated legumes are pigeon peas, common beans, mung beans, cowpeas, alfalfa, chickpeas, clovers, lentils, garden peas, lupins, and peanuts [179]. Gao *et al.,* reported that the soy lipophilic protein NPs act as an effective delivery vehicle for linoleic acid [180].

Legumin and vicilin NPs

Legumin is storage protein from *Pisum sativum. Mirshahi et al.,* [181] prepared legumin NPs of approximately 250 nm in size via a pH-coacervation protocol and chemical cross-linking with glutaraldehyde. However, this organic solvent-free preparation method yielded only approximately 27% of protein as NPs. In addition, no significant differences in size, percentage yield, or surface charge were observed between the legumin NPs cross-linked with different glutaraldehyde concentrations. The legumin NPs were quite stable in PBS, and they followed a zero-order degradation manner, whereby, a longer half-life (t50) was obtained with increasing glutaraldehyde concentrations. The amount of methylene blue (MB), used as a model of hydrophilic drug, loaded was approximately 6.2% of the initial dye. Its release from the NPs consisted of a rapid initial phase, followed by a slower second period, in which the rates in the second phase were inversely related to the degree of cross-linking.

Glycinin and β-conglycinin NPs

Soybeans (*Glycine max* L.) are currently one of the most abundant sources of plant proteins. The enriched form of soy protein, known as soy protein isolate (SPI), has been reported to unveil high nutritional values and desirable functionalities; its wide application as a food ingredient has been well documented. SPI also possesses a balanced composition of non-polar, polar, and charged amino acids; thus, drugs can be incorporated with its various functional groups. The major components of SPI are glycinin (MW = 360,000, ~ 60%) and β-conglycinin (MW = 180,000, ~ 40%). Teng *et al*.,[182] successfully encapsulated curcumin, as a model drug, into NPs, and the average size of the curcumin-loaded NPs ranged from 220.1 to 286.7 nm, and their zeta potential was approximately −36 mV. The highest encapsulation efficiency and loading efficiency achieved in their study were 97.2% and 2.7%, respectively.

3.2. Plant polysaccharide-based nanostructures

At first glance, the relationship between nanotechnology and lignocellulosic biomass may seem unrelated. However, it is important to recognize that, at a fundamental level, lignocellulosic biomass is comprised of nanoscale building blocks that provide valuable properties to wood and other types of renewable cellulosic and lignocellulosic biomaterials [183].

3.2.1. Cellulose nanostructures and lignocellulosic materials

Lignocellulosic materials are natural, renewable, readily available, environmentally friendly, biodegradable, and inexpensive resources with advantageous characteristics and significant importance to the industrial sector. The applications of these resources are necessary for the growth and progression of a sustainable economy worldwide [184]. There are some salient advantages of lignocellulosic fibers, in comparison to synthetic fibers: (a) the availability of a

wide variety of fillers worldwide; (b) renewability; (c) non-food agricultural economy-based product; (d) low density, cost, and energy consumption; (e) specific strength and modulus; (f) a reactive surface that can be employed to graft certain groups; (g) high sound attenuation of its composites; and (h) recyclability by combustion, as compared to inorganic filler systems [185].

The great potential of renewable biomaterials has been previously overlooked. Trees and plants use air, sunlight, and water to conduct processes in their "photochemical factories," and generously produce naturally occurring nanocomposites of cellulosic microfibrils embedded in a lignin matrix [186]. As a result of recent insight into this nature gift, the great potential of lignocelluloses as nanomaterials has come into limelight. Their unique nanocellulosic structure can be isolated by a top-down approach and custom-made into well-defined architectures that are sustainable, renewable, recyclable, and environmentally friendly [136].

3.2.1.1. Cellulose

Cellulose is a fibrous, semi-crystalline polymer of high molar mass and. is the most abundant biopolymer on earth [187], which is a renewable, carbon-neutral, biodegradable, sustainable, and inexpensive raw material (Figure 6). It is the main constituent of plant structures, where its extended chain conformation and microfibrillar morphology contributes to its significant load-carrying capability [137]. Cellulose is found in plants in the form of microfibrils, which comprise the structurally strong framework of cell walls; microfibrils are bundles of cellulose ($C_6H_{10}O_5$) molecules that are elongated and stabilized laterally by hydrogen bonds. A single microfibril contains multiple elementary fibrils consisting of many cellulose chains. The typical diameter of elementary fibrils is between 2 and 20 nm, and is reportedly affected by many factors, such as source, variety, soil, climate, harvest, maturity, etc. [188-192]. The Young's

modulus and tensile strength of cellulose nanofibrils has been reported to be approximately 145

GPa and 7.5 GPa, respectively [189, 193, 194], and the high modulus of the cellulose microfibril has

been attributed to the molecular alignment and dense packing in the unit cell [137].
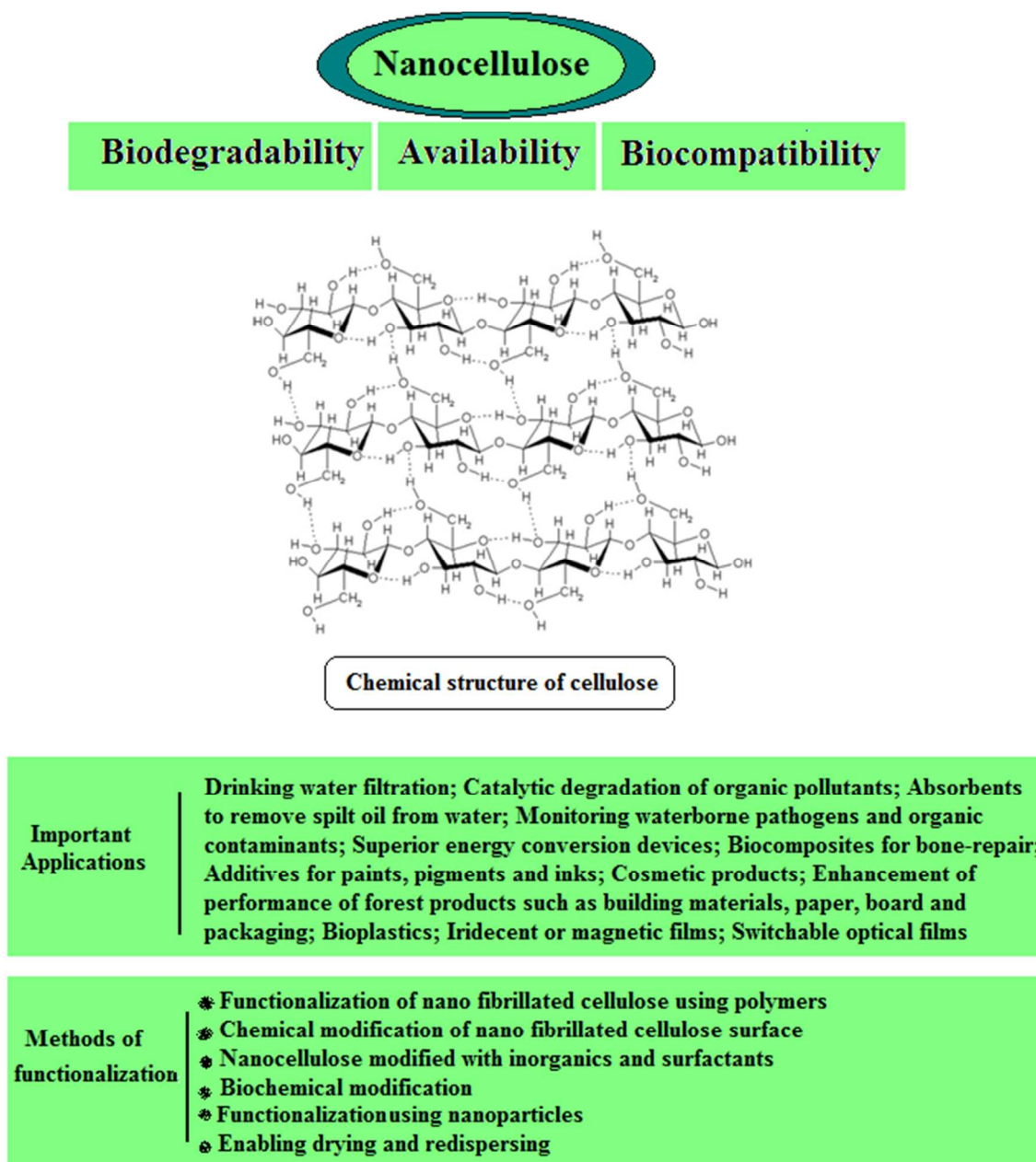
Figure 6. Nanocellulose and its important applications.

Nanocellulose possesses remarkable physical properties, special surface chemistry and excellent biological properties. Abundant availability, biodegradability, biocompatibility and low toxicity are the main advantages of nanocellulose. Nanocellulose-based nanocomposites have shown potential for applications in drinking water filtration, catalytic degradation of organic pollutants, absorbents to remove trickled oil from water, censoring organic contaminants and waterborne pathogens, and exceptional energy conversion devices. Nanocellulose exists in a number of forms such as that are commonly described as microfibrillated cellulose or nanofibrillated cellulose (homogenized cellulose pulps), nanocrystalline cellulose or cellulose nanocrystal (acid hydrolyzed cellulose whiskers), and bacterial cellulose (Figure 7). microfibrillated cellulose are often produced by high-sheer mechanical treatment of micron-sized cellulose pulp that has been pre-treated with bleaching agents to remove lignin and hemicellulose. Typical mechanical treatments incorporate refining and high pressure homogenization. In addition to mechanical homogenization, ultrasonic techniques have also been found to be useful for microfibrillated cellulose preparation. In one study, cellulose pulp was pretreated with endoglucanases before homogenization. The resultant nanocelluloses contained both 10-20 nm MFCs and 5 nm microfibrils. Because of the mild enzymatic hydrolysis prior to mechanical treatment, the required energy input was greatly reduced. Nanocrystalline celluloses are highly crystalline nanocelluloses with lower aspect ratios than microfibrillated celluloses that can be prepared by mineral acid hydrolysis of plant cellulose pulp, filter paper, and bacterial cellulose [195]. Nanocellulose and their properties have been reviewed comprehensively by Dufrense [196, 197].
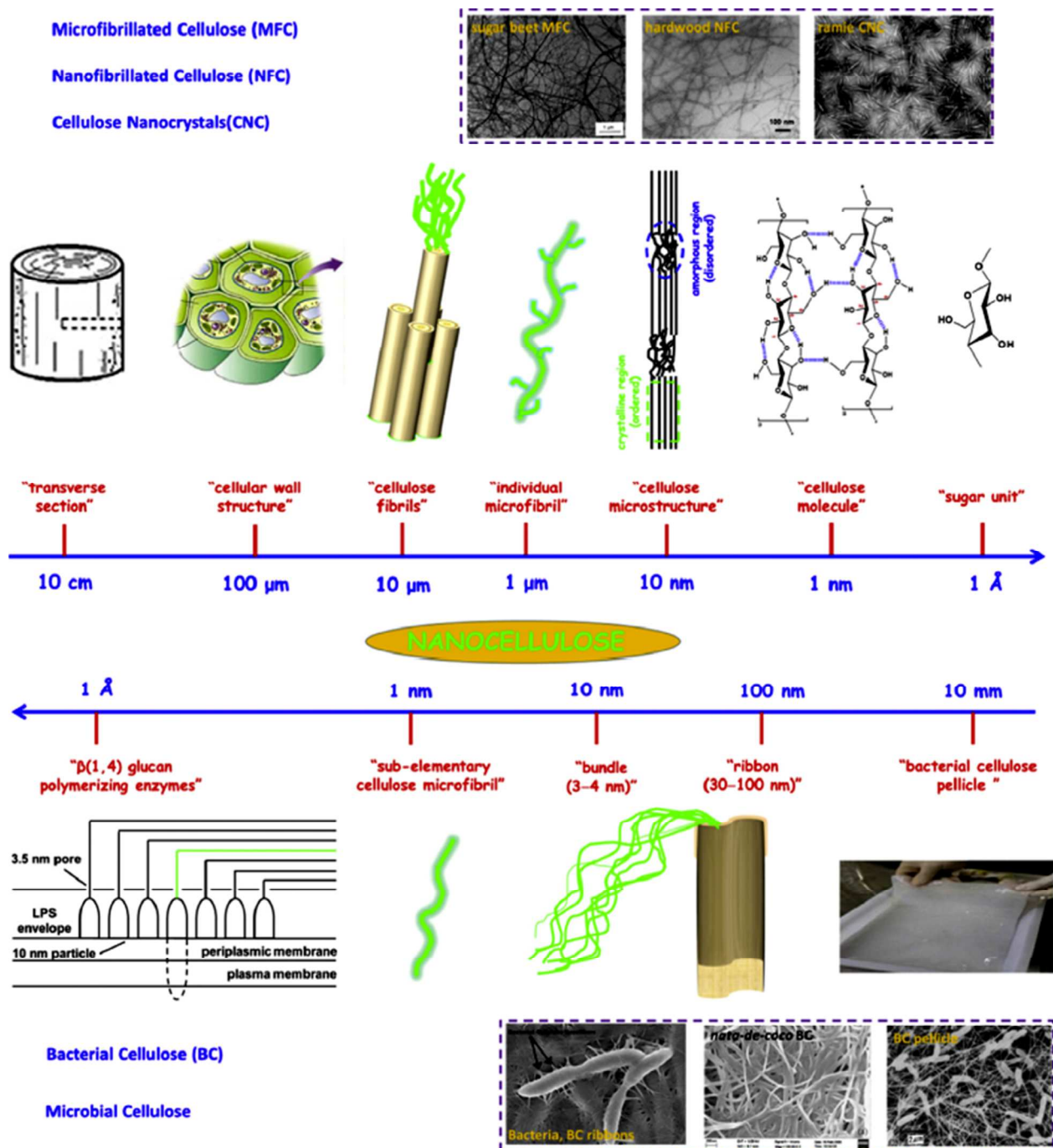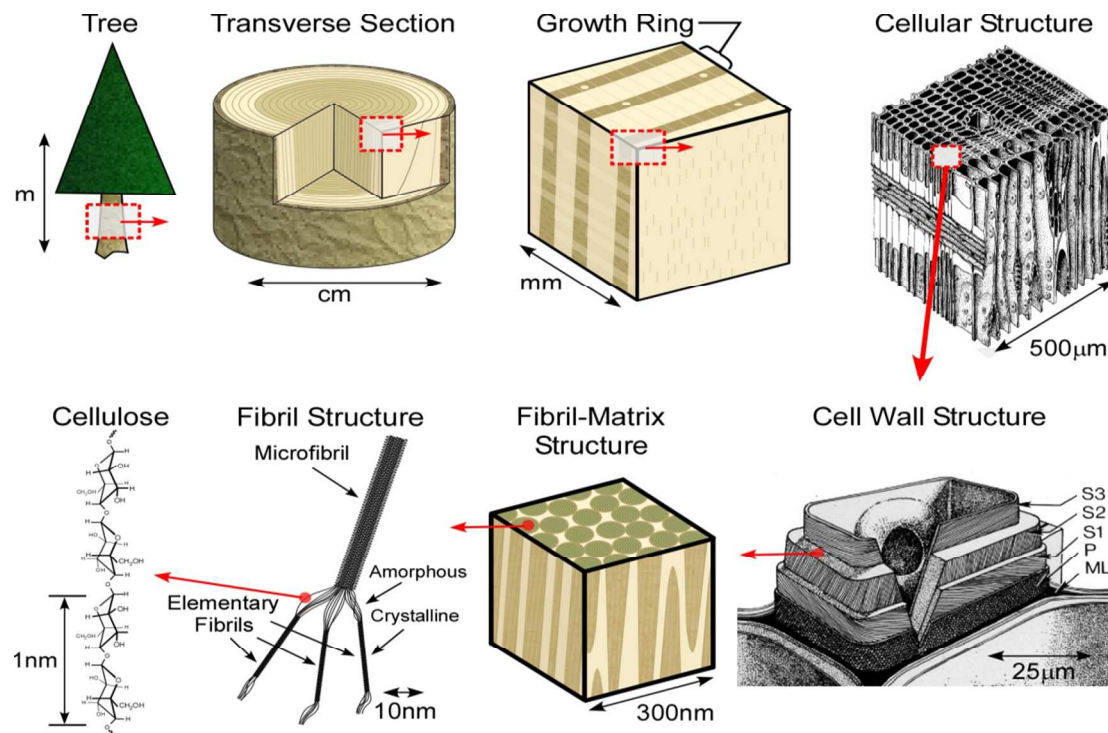
Figure 7. Hierarchical structure of cellulose; top image (from large unit to small unit): cellulose nanocrystals (CNC), micro/nanofibrillated cellulose (MFC and NFC); bottom image (from tiny unit to small unit): bacterial cellulose (BC). Transmission electron micrographs of sugar beet

MFC, hardwood MFC, ramie CNC, and scanning electron micrographs of BC ribbons, nata-de-coco BC, and BC pellicle. Reproduced with permission from ref [135]

Hierarchical structure

Natural fibers, such as wood, are cellular hierarchical bio-composites (Figure 8). At the nanoscale level, natural fibers are a cellulosic-fibrillar composite. Nanofibrils in their simplest form are elementary cellulosic fibrils, containing both crystalline and amorphous segments, and can be hundreds to a thousand nanometers long. This hierarchical structure, based on elementary nanofibrillar components, is responsible for the unique strength and high performance properties of different species of wood and natural fibers [186].

Nanotechnology provides the tool for isolating nanocelluloses from natural sources and most of the methodologies for the isolation of cellulose nanofiber require the use of a combination of chemical, mechanical, and other processes. The resultant cellulose nanofibers could have different morphologies, such as an entangled network (nanofibers) or rod-like NPs (whiskers). Increasing the crystallinity or reducing the amorphous region of fibers, by removing the hemicelluloses and lignin, has been shown to effectively increase the cellulose content, and as a result, the fibers had much higher strength. However, notably, lignin and hemicellulose removal could have detrimental effects in this regard, depending on how it is performed, as removal could lead to partial cellulose degradation [198]. The elastic moduli of solid wood, single pulp fiber, microfibrils, and crystallites were 10 GPa, 40 GPa, 70 GPa, and 250 GPa, respectively[199]. Thus, breaking down the cellulosic fibers to the micro- or nanoscale thus significantly improved the strength of the resulting fibers [200].

Figure 8. Schematic of the tree hierarchical structure and natural fibers. Reprinted with permission from ref [198].

3.2.1.2. Potential sources

Wood-based resources

Wood-based resources can be used as a source of cellulose and for nanocellulose isolation. Cellulosic nanofibers have been successfully isolated from wood using a combination of chemo-mechanical treatments [201-203].

Non-wood crops

There are several advantages in using agricultural residues and natural fibers, over wood-based resources, because wood is valuable commodity for use in the construction and furniture industries, as well as in the pulp and paper sector. These demands place increased pressure on

wood supplies for nanocellulose production, and as such, interest in agricultural residues and natural fibers e.g., flax, hemp, jute, kenaf, sisal, and others, has grown. The other advantages of using plant fibers include the pace of their renewability in comparison to wood, reduced lignin content that makes them easier to process and defibrillate with decreased energy demand is another salient feature [204].

Researchers have used various agricultural residues as sources for nanocellulose production, e.g., rutabaga [205], wheat straw [206, 207], bamboo [208], potato tubers [209], hemp [210, 211], soybean stock [212], sugar beet pulp [213-216], bagasse [217, 218], sugarcane bagasse [219], cottonseed linter [220], flax [221], ramie [222], pea hull [223, 224], kenaf [136, 200, 225-229], wheat straw and soy hulls [230], oil palm empty fruit bunch [230-232], swede root [233], sisal [234], jute [235, 236], banana rachis [237], rice husk [238, 239], coconut husk [240, 241], and Mengkuang leaves [242].

Bacterial source

Certain bacteria, belonging to the genera *Acetobacter*, *Agrobacterium*, *Alcaligenes*, *Pseudomonas*, *Rhizobium*, or *Sarcina* [243], biosynthesize cellulose or secrete cellulosic fibers extracellularly. There are several morphological differences between bacterial cellulose and extracted nanocellulose from wood or plants, e.g., it produces ribbon-shaped fibrils, less than 100 nm wide, which are composed of much finer 2–4 nm nanofibrils [244, 245]. Celluloses produced from bacteria offer certain exceptional properties, such as fine and pure fibrous network structure, as well as greater mechanical strength; bacterial cellulose has been used as a source of nanocellulose [246-254].

3.2.1.3. Isolation techniques for nanocellulose

Isolation of cellulosic nanofibers or crystalline whiskers usually requires a multi-stage process involving vigorous chemical and/or mechanical procedures. Lignin impedes the separation of wood into its component fibers, so it is reasonable to consider delignification methods as promising initial steps for the preparation of nanocellulose [255]. These chemical processes aim to produce purified cellulose, such as bleached cellulose pulp, which can then be further processed. Wood pulp, prepared by chemical methods, can be defibrillated by various mechanical methods or further, via acidic hydrolysis. These techniques are discussed in detail below.

Mechanical approaches

Homogenizing: This process occurs in a special homogenizing valve, which is the heart of the equipment, wherein the fluid passes through a gap in the homogenizing valve. This creates conditions of high turbulence and shear, combined with compression, acceleration, pressure drop, and impact, which causes the disintegration of particles [256]. For this purpose, a diluted suspension of refined cellulosic fibers is fed into the machine and to achieve nanoscale cellulosic fibers, this homogenization process must be repeated several times which varies significantly throughout the literature. This inconsistency could be due to the degree of pre-treatment and refining processes performed prior to the homogenization process, the raw material used, the fiber length, and the applied pressure. For example, Jonoobi *et al*., [226] reported the isolation of nanofibers from kenaf bast by using a homogenization process with 40 cycles at 500 bar, while Iwamoto *et al*., [257] reported 14 times as an optimum number of repetitions, and described that further repetitions up to 30 cycles did not improve fibrillation. Malainine *et al*., [258] also reported

that 15 cycles at 500 bar was enough for defibrillating the fibers to nanoscale dimensions. Overall, most researchers have subjected the fibers through the homogenizer approximately 10-20 cycles [259-262], with a common disadvantages of this mechanical treatment being the high energy demand and other issues associated with system clogging due to the processing of long fibers.

Cryocrushing: Cryocrushing is a technique presented by Chakraborty *et al*., [201] where the water in pulped fibers was frozen using liquid nitrogen, and high shear forces were then applied to force disintegration of the fibrils from the cell wall. Application of high impact forces to the frozen fibers by ice crystals exerts pressure on the cell walls, causing them to rupture, which leads to liberation of the microfibrils [212]. The nanofibers from wheat straw and soy hulls have been extracted by a mechanical approach involving cryocrushing[230], a process also used this technique to isolate nanoscale cellulosic fibers from chemically treated hemp, rutabaga, and flax fibers, and attained nanofibers with diameters ranging from 5–80 nm[263]. Wang and Sain., [212, 264] combined this technique with high-pressure homogenization to extract nanofibers from soybean stock with nanofibers with diameters ranging from 50 to 100 nm. The main disadvantage is the non-scalability of this method and since this method does not produce very fine fibrils, it is limited to cellulose fibrils from primary cell walls [265].

Grinding or microfluidization: In this method, a suspension of cellulosic pulped fibers is passed through a static grindstone and a rotating grindstone, revolving at high speed, *e.g.,* 1500 rpm [265, 266]. The fiber's cell wall, consisting of nanoscale building blocks and hydrogen bonds, is broken down by shearing forces generated by the grinding stones, which leads to liberation of nanoscale cellulosic fibers. Karimi *et al*., [136] obtained nanofibers from kenaf bast with diameters

ranging from 2.2–34 nm by using this technique. When homogenized cellulosic pulp was subjected to a grinder treatment, the fibril bundles were further fibrillated and 10 repetitions of the grinder treatment resulted in uniform nanofibers that were 50-100 nm wide[257, 267].

In contrast with homogenization, processing of cellulosic fibers with a microfluidizer reduces the likelihood of clogging because it has no in-line moving parts [265], and if clogging occurs, it can be resolved by using reverse flow through the chamber. The main disadvantage of microfluidization has been the maintenance of the disk and disk replacement since wood pulp fibers can rapidly wear down the grooves and grit. However, a primary advantage is that the mechanical fiber shortening pre-treatment, utilized with other processing techniques, may not be required.

Pre-treatments

Mechanical approaches for nanocellulose isolation have two drawbacks, including high-energy consumption and long fiber lengths that cause clogging of the equipment. Mechanical, chemical, and enzymatic pre-treatment processes can significantly decrease the energy consumption and reduce fiber size, thereby reducing the frequency of equipment clogging. *Mechanical pre-treatment*: Mechanical reduction of fiber size can be performed using PFI mills, valley beaters, manual cutting, and disk refiners. Usually these pre-treatment methods are used prior to the production of nanofibers, i.e., prior to homogenization or microfluidization process [256, 257, 268].

Alkaline chemical pre-treatment: Alkaline pre-treatment is the most commonly used technique, as it promotes fiber swelling that makes the defibrillation process easier and less energy consuming. Several researchers have used alkaline pre-treatment prior to the main

defibrillation process [211, 212, 214, 226, 228, 242, 264, 269, 270]. The purpose of the alkaline treatment is to dissolve and eliminate lignin and hemicellulose from the matrix surrounding the cellulose microfibrils, rendering them vulnerable for isolation of individual microfibers. However, the process needs to be carefully controlled to avoid undesirable cellulose degradation [212, 263]. Abe *et al*., [266] produced nanofibers from wood powder, with only one pass through a grinder, following extensive chemical pre-treatment. *Oxidative chemical pre-treatment*: Oxidation pre-treatment, also known as a TEMPO-mediated oxidation process, deploys radicals emanating from 2,2,6,6-tetramethylpi-peridine-1-oxyl (TEMPO) on the substrate prior to the main defibrillation treatment; this technique has proven promising for the surface modification of native celluloses [216, 271-276]. Uniform nanofibers with diameters of 1-5 nm have been isolated via oxidation using nitroxyl radicals from TEMPO [277] and nanofibers possess the same crystallinity as the starting materials; [276] when used in conjunction with mechanical treatments, over 90% yield was achieved[278]. Cellulose nanocrystals and nanofibrils could be generated from pure rice straw cellulose via sulfuric acid hydrolysis, mechanical blending, and TEMPO-mediated oxidation[279]. Interestingly, the TEMPO-mediated oxidation procedure produced the most uniform and finest (approximately 1.7 nm) nanofibers, but the nanofibers were found to be the least crystalline.

Enzymatic pre-treatment: Cellulose enzymes have been suggested to favor the attack on the amorphous region of the cellulosic substrates, making it easier to separate the material into microfibrillated cellulose. A reduction in energy demand has been observed when enzymatic pre-treatment was applied prior to the mechanical treatments[268, 280, 281]. The isolation of cellulose microfibrils by treating bleached kraft pulp, using enzymatic approaches, led to a significant reduction in fiber diameters [282]; nanofibers from wood, subjected to enzymatic pre-treatment, resulted in a more favorable structure than wood subjected to strong acidic hydrolysis[283].

Acid hydrolysis: Cellulose fibers and microfibrils do not display a regular surface, i.e., apart from the crystalline domains, cellulose also occurs in a non-crystalline or amorphous state; amorphous regions are randomly oriented in a spaghetti-like arrangement, leading to a lower density in comparison to nano-crystalline regions [284, 285]. The amorphous regions are susceptible to acid attack and, under controlled conditions; they may be removed, leaving crystalline regions intact [286]. Strong acid, usually sulphuric acid, is used to hydrolyse cellulose by which is immediately followed by quenching the reaction with deionised water. In order to attain higher concentration of the cellulose and to remove extra aqueous acidic solution,, the suspension is centrifuged. Cellulosic nanocrystals from kenaf [228, 229], bagasse [218], cottonseed linter [220], cotton [287], flax [221], hemp [210], ramie [222], pea hull [223, 224], and tunicate [288-290] have been isolated by using this acidic hydrolysis.

3.2.2. Starch Nanostructures

Starch, is a renewable and biodegradable polymer that is produced by many plants to reserve carbohydrates (Figure 9). In addition to wood and natural fibers, starch has been a commonly selected material since the inception of human technology [291]. Starch-based materials are now considered the most promising sustainable materials for the production of biodegradable plastics [292]. Furthermore, total starch production from major crops is estimated to be at 81 million tons by 2015, with corn starch comprising the majority of this quantity.

Starch granules have 3D architecture with varying crystallinity from 15% to 45% [293], and consist of d-glucose units with two major biomacromolecules, including amylose and amylopectin (Figure 10). Amylose is a sparsely branched carbohydrate while, amylopectin is a highly multiple-branched polymer, with a high molecular weight responsible for the materials'

crystallinity [294]. Depending on the source, the amylose content of starch can vary from less than

1% to 83% [295], and its content can significant affect the thermal, rheological, and processability

of starch-based materials [296, 297].
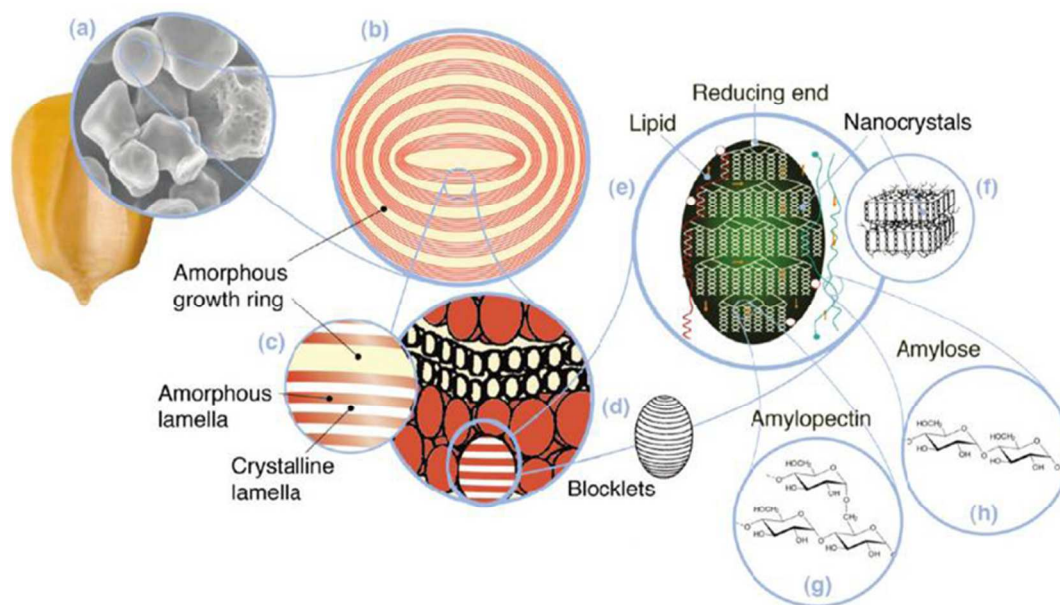
Figure 9. Starch multiscale structure: (a) starch granules from normal maize (30 μm), (b)

amorphous and semicrystalline growth rings (120-500 nm), (c) amorphous and crystalline

lamellae (9 nm), magnified details of the semicrystalline growth ring, (d) blocklets (20-50 nm)

constituting a unit of the growth rings, (e) amylopectin double helixes forming the crystalline

lamellae of the blocklets, (f) nanocrystals: other representation of the crystalline lamellae called

starch nanocrystals when separated by acid hydrolysis, (g) amylopectin's molecular structure,

and (h) amylose's molecular structure (0.1-1 nm). Reproduced with permission from ref [298].
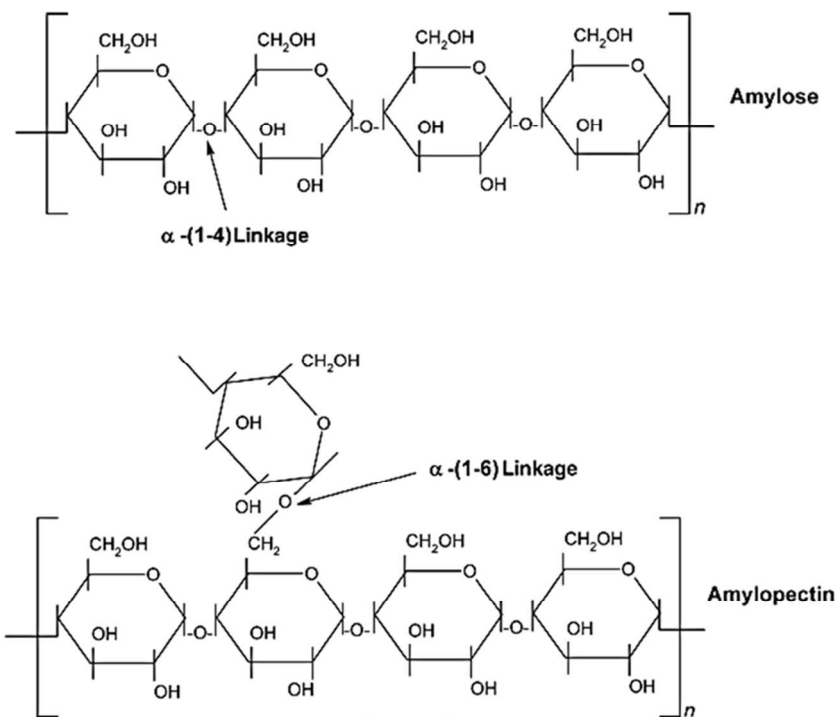
Figure 10. Chemical structure of starch with amylose and amylopectin units. Reproduced with permission from ref [292]

Starch nanocrystals

Starch crystallite, starch nanocrystal, microcrystalline starch, and hydrolyzed starch all stand for the crystalline part of starch obtained by hydrolysis, but to a different extent [298]. Initial interest in starch nanocrystals was triggered in 1996 by Dufresne *et al.*, [299] when they described the isolation of microcrystalline starch with diameters in the range of a few tens of nanometers via acidic hydrolysis. Later in 2003, Putaux *et al.*, [300] extracted nanocrystals with diameters of 15-30 nm and lengths between 20-40 nm from waxy maize starch by acid hydrolysis. Recently, the isolation of starch nanocrystals from potatoes [301-303], peas [304, 305], and waxy maize [306-308] has been reported, while the diameter of nanocrystals has been shown to vary within the range of 40-150 nm; this variation could be due to starch source and its botanical origin [309].

3.2.2.1. Preparation techniques for starch nanocrystal

There are two prevailing processes for starch nanocrystal isolation, regardless of starch type and the origin and both techniques are based on acidic hydrolysis; the first method introduced by Dufresne *et al*. [299] involved hydrolysis by hydrogen chloride while the second method was described by Angellier *et al*., [310] and used hydrolysis by sulfuric acid. A schematic of different pathways for producing crystalline and amorphous starch NPs is depicted in figure 11.
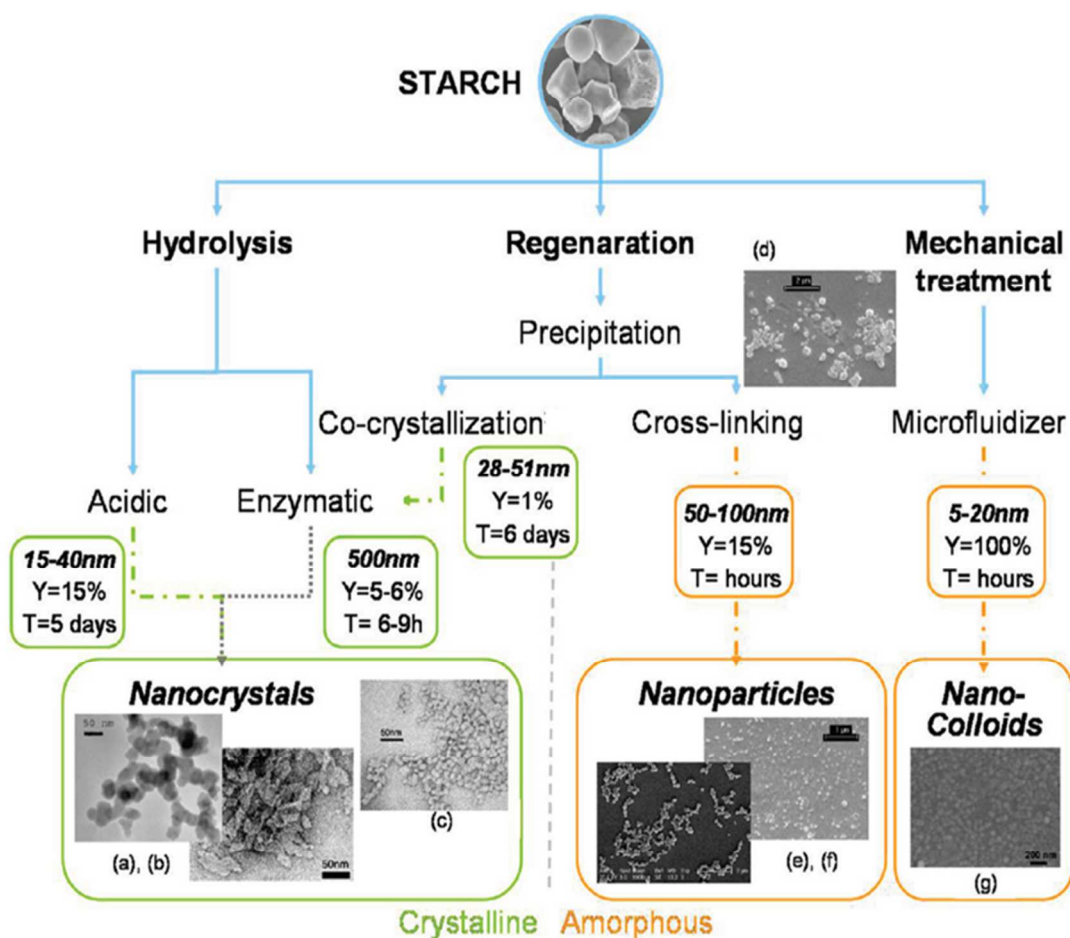
Figure 11. Different ways of producing crystalline and amorphous starch NPs: hydrolysis leads to nanocrystals, whereas regeneration and mechanical treatment lead to both amorphous and

crystalline particles in the final batch. (a) TEM micrograph of starch nanocrystals , (b) TEM micrograph of starch nanocrystals. Enzymatic hydrolysis is used to selectively keep crystalline particles: (c) TEM micrograph of starch nanocrystals after cocrytallisation and enzymatic hydrolysis. The production of starch NPs by precipitation of gelatinized starch in nonsolvent followed by a cross-linking reaction: (d) precipitated starch NPs before cross-linking , (e) starch NPs and (f) citric acid cross-linked starch NPs. By analogy with microfibrillated cellulose (MFC): (g) TEM micrograph of starch nanocolloid. Reproduced with permission from ref [298].

Compared to cellulose nanocrystals, the reinforcing capacity of starch nanocrystals is rather limited. Consequently, it should be used in higher amount to reach similar reinforcing effects. However, other interesting properties can be obtained from their platelet-like morphology like barrier properties. Yet another limitation of starch nanocrystals is the length of the hydrolysis process which is much longer than for cellulose and need to be performed at lower temperature owing to the higher sensitivity of starch to the acid assault [298].

3.2.3. Current challenges

Despite the abundance of available cellulose worldwide as a raw biomaterial, its utilization as a common industrial component is still in its early stages, yet offers great potential for the future. When considering the high Young's modulus of cellulose, one may wonder why cellulose microfibrils have not already been disintegrated from plant structures, and used commercially in structural materials. Reportedly, there are problems regarding the compatibility of the fiber-matrix composite, which typically reduces the mechanical properties of composites. For this reason, surface treatments are usually required to enhance the association between the fiber and matrix. The mechanical properties and adhesion of natural fibers in reinforced plastic,

such as polypropylene/flax, epoxy/flax, and polyester/kenaf, have been enhanced using chemical treatment processes. Among others, distribution of cellulose nanofibers in a polymer matrix poses a major problem to this particular process. Moreover, significant contact between these nanofibers could be produced by the high density of hydroxyl groups at their surfaces, and cause them to agglomerate.

The low thermal stability is yet another restricting factor that limits the use of lignocellulosic fibers in material composites. To avoid fiber degradation during processing, the temperature is limited to 200 °C, which further restricts the choice of the polymer matrix materials. Moreover, studies on the use of laboratory-scale processing methods such as solution casting has illustrated cellulose nanocomposites in terms of their morphological, physical, and mechanical properties. However, the developments of new industrially viable processing techniques are crucial to promote the commercial applications for these materials.

In contrast to the cellulosic nanostructures, significantly fewer studies evaluating starch nanocrystals are available. One of the main interests for use of starch, in addition to a low cost, is that the raw material is relatively pure and does not need intensive purification procedure such as lignocellulosic materials[298]. Consequently, in view of the lower crystallinity of starch nanocrystals than that of nanocelluloses, their reinforcing potential is lower and they need to be used in higher amounts to attain similar reinforcement effects. However, their unique platelet-like morphology introduces some valuable features, such as barrier properties. The disadvantage of starch nanocrystals is that their isolation requires a much longer hydrolysis time in comparison to cellulose.

3.2.4. Potential applications

The potential of nanocelluloses is determined based on their mechanical properties as a nano-reinforcing phase, and their advanced functional applications are based on their other unique properties. The concept of cellulose nanocomposites for load-bearing applications, however, is fairly new. When compared to lignocellulosic microcomposites, enhanced properties, due to the higher Young's modulus of pure cellulose reinforcement and more finely distributed reinforcing microfibrils, are expected. Both cellulose and starch nanostructures have a small diameter, large aspect ratio, biocompatibility, and high strength and modulus, in addition to other favorable physical properties associated with the highly crystalline extended chain conformation. Excluding the composite industry, there are many other businesses wherein cellulosic nanostructures have important applications, *e.g.,* electronics (flexible circuits), energy (flexible batteries, such as Li-ion batteries and solar panels), packaging, coatings, detergents, adhesives, construction, inks and printing, pulp and paper, filtration, and life science (scaffolds in tissue engineering, artificial skin and cartilage, wound healing, and vessel substitutes), optical devices (including reflective properties for security papers and UV or IR reflective barriers), rheological modifiers, and cosmetics [196,311].

Moores *et al.,* [312] demonstrated an unprecedentedly high enantiomeric excess for Pd NPs deposited onto cellulose nanocrystals which has used as catalysts for the hydrogenation of prochiral ketones in water at room temperature; cellulose nanocrystals served as support and sole chiral source, delivering an enantiomeric excess of 65% with quantitative conversions via

binding of Pd NPs onto cellulose nanocrystals thus providing an insight into the chiral induction mechanism.

3.3. Carbon-based nanostructures from plants

Carbon is the essential and abundant universal chemical element with several allotropic forms with unique properties. The best-known forms are amorphous carbon, graphite, diamond, and fullerenes. Approximately 1,900 gigatons of elements are present in the biosphere and form the basis of all known life on Earth, and without these elements, life could not exist. Carbon can form very vital bonds with hydrogen and oxygen to build carbohydrates and various other groups of important biological compounds. When associated with nitrogen, sulfur, and phosphorus, carbon forms amazing and infinite biomolecules, including lipids, alkaloids, antibiotics, amino acids, DNA, RNA, ATP, lignans, chitins, alcohols, fats, aromatic esters, carotenoids, terpenes, and rubber products. Plants draw carbon dioxide from their environment and use it to build biomass, as in carbon respiration or the Calvin cycle, a process of carbon fixation. Plants, therefore, are the key carbon source for producing carbon nanostructures [138].

Several researchers have prepared carbon-based nanostructures from plants [313-316]. Wang *et al.,* [317] used microwave (MW)-assisted pyrolysis to fabricate porous carbon nanostructures from biomass precursors (*e. g.,* wood, cotton, and filter paper) filled with a conducting polymer and iron (Fe) catalytic species. The morphology and porosity of the biomass precursors were retained, but their infrastructure became highly graphitic after the MW irradiation treatment. The conducting polymer served as the MW absorbent, while the Fe species catalyzed the polymerization of pyrrole in the first step, as well as expedited pyrolysis of the biomass precursor during MW irradiation. The ensuing graphitic carbon materials possess relatively high

surface areas and openly accessible pores. The building blocks of the porous materials have changed from natural polymer tissues to various graphitic carbon nanostructures, including nanofoams, nanoflakes, nanoribbons, and sponge-like nanosheets. Saxena and Sarkar [318] isolated carbon NPs (CNPs) from bread. A simple oxidative treatment rendered them water-soluble and fluorescent, and the CNPs exhibited fluorescence over a broad range of excitation wavelengths and have been successfully used for fluorescence imaging of human erythrocytes under 488- and 561-nm band pass filters. Upon direct interaction with human erythrocytes, these CNPs showed ~6% hemolysis in 5 h. In the presence of blood plasma, the quantum yield of these water-soluble CNPs was enhanced from 2% to 4.5%, giving rise to a new phenomenon of auto passivation of CNPs by bio-fluids.

Muramatsu *et al.*, [139] demonstrated a new synthesis method for transforming rice husks into bulk amounts of graphene via calcination and chemical activation. The bulk sample comprise crystalline nano-sized graphene and corrugated individual graphene sheets; the material generally contains one, or more layers, and corrugated graphene domains were typically observed in monolayers containing topological defects within the hexagonal lattice and edges. Both types of graphene's exhibit atomically smooth surfaces and edges.

The oral ingestion of a fluorescent probe is a novel approach for imaging living species. Ghosh *et al.*, [319] have introduced water-soluble carbon nano-onions (wsCNOs) as a non-toxic, fluorescent reagent enabling live imaging of *Drosophila melanogaster* (fruit flies). Water-soluble CNOs, synthesized from wood waste, colorfully image all the developmental phases of *Drosophila melanogaster*, from the egg to adulthood. Oral ingestion of up to 4 ppm of soluble CNOs allowed optical fluorescence microscopy imaging of all stages of the fruit fly life cycle

without exhibiting any toxic effects; fluorescent *Drosophila melanogaster* excrets this fluorescing material upon the removal of the CNOs from its food. Sonkar *et al*., [320] reported the *in vivo* effects of wsCNOs introduced in the common food web of two model organisms: unicellular *E. coli* and multicellular *Caenorhabditis elegans*. At first, CNOs were fed to *E. coli*; subsequently, the *E. coli* were fed to *C. elegans*. The wsCNOs were found to serve as a highly fluorescent bio-imaging agent and the results did not indicate any toxic effects caused by the wsCNOs on the growth of these organisms.

Sonkar *et al*., [321] reported that wsCNOs isolated from wood wool, a wood-based pyrolysis waste product of wood, enhanced the overall growth rate of gram (*Cicer arietinum*) plants. Treatment of plants with up to 30 μg mL^{-1} of wsCNOs for an initial 10-day period under laboratory conditions led to an increase in the overall growth of the plant biomass. Analysis of the carbon, hydrogen, and nitrogen content for the shoot and fruit sections of the plants, treated with and without the wsCNOs, showed only a minor difference in the compositions. However, a slight increase in the percentage of carbon and hydrogen in the shoots reflects the synthesis of more organic biomass in the treated plants.

3.3.1. Carbon nanotubes (CNTs)

CNTs are seamless cylinders of one or more layers of graphene (denoted as single-wall, SWNT, or multi-wall, MWNT), with open or closed ends. Perfect CNTs have all carbons bonded in a hexagonal lattice, except at their ends, whereas defects in mass-produced CNTs introduce pentagons, heptagons, and other imperfections in the sidewalls that generally degrade the desired properties. SWNTs and MWNTs have diameters of typically 0.8-2 nm and 5-20 nm, respectively, although the diameters of MWNTs can exceed 100 nm. The length of CNTs range

from less than 100 nm to several centimeters, thereby bridging the molecular and macroscopic scales [322]. CNTs are increasingly used in many applications due to their unique electrical, mechanical, optical, thermal, and other properties [323]. The application of CNTs is determined based on the CNTs structure (number of walls, diameter, length, chiral angle, etc.), which imparts them with specific properties. The potential applications of CNTs include conductive films, fuel cells, solar cells, transistors, supercapacitors, sensors, displays, separation membranes and filters, purification systems, and clothes, etc. Large quantities of CNTs may be produced using various methods. Chemical vapor deposition (CVD) is the dominant method for high-volume CNT production, and typically utilizes fluidized bed reactors that enable uniform gas diffusion and heat transfer to metal catalyst NPs.

Chen *et al*., [140] reported the synthesis of carbon nanofibers on activated carbons produced from agricultural waste using chemical vapor deposition. Importantly, Fe already present in the ash content of the activated carbon was employed as a natural catalyst for nanofiber formation, and the need for a wet chemical catalyst preparation step was thus avoided. Notably,Zhu. *et al*., [141] reported the synthesis of MWNT from bamboo charcoals by chemical vapor deposition in the presence of ethanol vapor; Mg_2SiO_4 and, particularly, calcium silicate were responsible for the nucleation and growth of CNTs at 1200 °C-1400 °C. TEM and EDS examinations showed that the tips of nanotubes synthesized at 1200 °C-1400 °C consisted mainly of calcium silicate, thereby acting as effective catalysts for the nucleation of nanotubes. The CNT formation was found to occur following the vapor-liquid-solid (VLS) mechanism, which includes initial decomposition of ethanol vapor into carbon, dissolution of carbon inside molten silicate, and final nucleation of CNTs. Furthermore, the upload of CNTs in bamboo charcoals markedly increased the specific surface area from 98 to 655 $m^2\,g^{-1}$ and the adsorption capacity from 0.05 to

0.35 cm^3 g^{-1}. The CNT growth by silicate may permit applications in cement, in which the production temperature is normally ~ 1450 °C, and the silicate inside the cement could be a catalyst for the growth of CNTs.

Goodell *et al.*, [324] reported the synthesis of CNTs from wood fiber using a low-temperature process, which included continuous oxidation at 240 °C and cyclic oxidation at 400 °C; the inside diameter of the ensuing CNTs was ~ 4-5 nm while the outside diameter ranged from 10-20 nm. In contrast, no CNTs were produced when pure lignin and cellulose were evaluated, indicating that the molecular and spatial arrangement of the cell wall played an important role in CNT formation. This study suggested that the chemical components in the secondary plant cell wall, and their differential ablation properties, were critical for the formation of CNTs at these comparatively low temperatures.

Sustainability of any civilization depends on its energy resources, and the technological capital for their conversion and conservation. Paul *et al.*, [325] reported the synthesis of CNTs from plant-based precursors and their application in organic photovoltaic cells and bio-diesel storage. Ye *et al.*, [326] reported the synthesis of a series of carbon nanostructures via a biotemplating method by catalytic decomposition of bamboo impregnated with ferric nitrate. The natural nanoporous bamboo was used as both a green carbon source and a template for the *in situ* growth of carbon nanostructures; SEM, field emission TEM, and EDS were used to characterize the product. Four distinct structural types of carbon nanostructures were identified, namely nanofibers, hollow carbon nanospheres, herringbone, and bamboo-shaped nanotubes. The effect of reaction temperature (600 °C-900 °C) on the growth behavior of carbon nanostructures was investigated, and the corresponding growth mechanism was proposed. The production of

nanofibers was favored at low temperatures, while higher temperatures led to bamboo-shaped nanostructures.

Xie *et al*., [327] produced CNTs from plant materials using a cyclic oxidation process, after the raw materials were pretreated by oxidative carbonization in air at ~ 240 °C. The cyclic oxidation process was found to be more effectual than a continuous heating process in ablating the residual carbon from cellulose. The results also indicated that no CNTs were produced unless a pre-oxidation process was used, or when the cyclic oxidation temperature increased above 600 °C. In another study, Zhao *et al*., [328] used black Jew's-ear fungus and black sesame seeds as catalyst precursors to prepare CNTs by chemical vapor deposition. Each catalyst particle rose from the metal content of a single cell of the precursor, hence the distribution of catalyst particles was uniform; their size and composition were almost identical. CNT arrays grew when black sesame seeds were used as catalyst precursors. CNTs with diameters of 80 nm and lengths greater than 100 μm grew when black Jew's-ear fungus was used.

Dubrovina *et al*., [329] reported the one-pot synthesis of CNTs by pyrolysis of the cellulose acetate (CA) cross-linked with polyisocyanate in a fumed silica template; $NiCl_2$ was chosen as the pre-catalyst for CNT growth. The diameter of the generated CNTs was 24-38 nm, and their wall thickness was 9-11 nm. The primary role of the CA pyrolysis in the formation of CNTs may be the combination of closed macropores in the template formed by evolved CO_2 during the cross-linking reaction and mesopores formed by silica particles; macropores acted as microreactors, while the mesopores templated the catalytic NPs. The importance of this method for CNT synthesis is based on the utilization of a readily available renewable resource of CA.

The technologically simple and energetically efficient method can be performed in a conventional tube furnace and did not require preliminary synthesis of a catalyst.

3.3.2. Carbon dots

Carbon nanodots (C-dots) are a new fascinating class of carbon nanomaterials with sizes below 10 nm and were initially reported in 2004 during the purification of SWNTs via preparative electrophoresis (Figure 12) [330]. C-dots have drawn significant attention due to their excellent photostability, favorable biocompatibility, low toxicity, outstanding water solubility, high sensitivity and excellent selectivity for target analytes, tunable fluorescence emission and excitation, high quantum yield (QY), and large stokes shifts. A variety of synthesis methods have been developed for C-dots including laser ablation, electrochemical oxidation, combustion/thermal MWA heating, and supported synthesis; however, some of these methods require complex equipment or treatment processes. Due to their inexpensive nature and simple operational steps, hydrothermal, solvo-thermal, and MWA synthesis methods have emerged among successful processes [331].
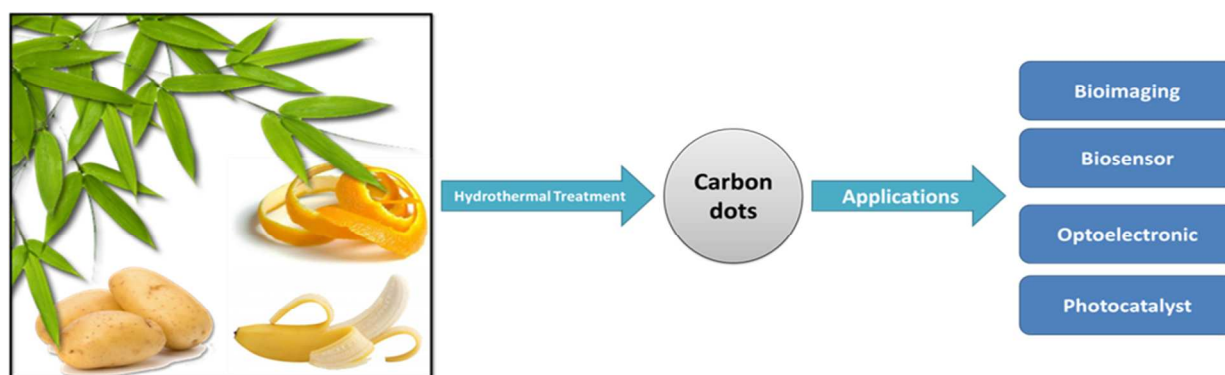
Figure 12. Carbon dots and their potential applications.

Green luminescent water-soluble oxygenous C-dots with an average size of 3 nm have been synthesized by simply heating banana (*Musa acuminata*) juice at 150 °C for 4 h, without using any surface passivating and oxidizing agent, or inorganic salt[332]. The ensuing C-dots offered an excitation wavelength and pH-dependent luminescent behavior in the visible range; the quantum yield was 8.95 on excitation at a wavelength of 360 nm, using quinine sulfate as the reference. In another study, dual-emission C-dots have been prepared via pyrolysis and MWA treatment of naked oats, providing a novel and sustainable pathway for the production of dual luminance C-dots without the requirement of tedious synthetic methodology or the use of toxic/expensive solvents and starting materials [333]; their intriguing dual fluorescence behavior comes to lime light at the excitation wavelength of between 250 and 310 nm. The well-resolved dual emission bands manifest excitation and temperature dependence. The produced C-dots were applied as a ratiometric fluorescent sensing platform for precise and quantitative detection of Al^{3+} ions and pH values, and as optical nanoprobes for cellular imaging.

Highly photoluminescent C-dots with a photoluminescence quantum yield of 26% have been prepared in one step via hydrothermal treatment of orange juice[334]. Due to their higher photostability and low toxicity, these C-dots were shown to be excellent probes for cellular imaging. A green and sustainable strategy for synthesizing nitrogen-doped C-dots has been reported via hydrothermal treatment of willow leaves[335]. The supernatant exhibited strong blue fluorescence under UV radiation, and could be directly used as a fluorescent ink. The solid product obtained via pyrolysis showed excellent electrocatalytic activity for a highly efficient oxygen reduction reaction with great stability, in addition to methanol/CO tolerance that was superior to a commercial Pt/C catalyst.

A simple, economical, and green method for preparation of water-soluble, fluorescent carbon NPs (CPs) has been reported with a quantum yield of approximately 6.9% via hydrothermal process using inexpensive waste from pomelo peel as a carbon source[336]. The use of such CPs was explored as probes for a fluorescent Hg^{2+} detection application, which was based on Hg^{2+}-induced fluorescence quenching of CPs; sensing system exhibited excellent sensitivity and selectivity toward Hg^{2+}, with a detection limit as low as 0.23 nM. In another greener and low-cost study, water-soluble fluorescent C-dots were prepared under hydrothermal conditions, with *Jinhua bergamot* plant as a carbon source [337]. The as-synthesized C-dots have better stability and relatively high photoluminescence with a quantum yield of 50.78%, along with the fluorescence lifetime of ca. 3.84 ns. These C-dots can be used for sensitive and selective fluorescent detection of Hg^{2+} and Fe^{3+}.

Mewada *et al.*, [338] reported the use of an economical, plant-based method for the production of luminescent water-soluble C-dots, using peel extract of Indian water plant (*Trapa bispinosa*) without adding any external oxidizing agent at 90 °C. C-dots (approximately 5-10 nm) were found in the solution with a prominent green fluorescence under UV-light (λ_{ex} = 365 nm). The UV-vis spectra recorded at different time intervals (30-120 min) displayed signature absorption of C-dots between 400 and 600 nm. Fluorescence spectra of the dispersion after 120 min of synthesis exhibited characteristic emission peaks of C-dots when excited at 350, 400, 450, and 500 nm. The C-dots structure was found to be turbostratic when evaluated using X-ray diffraction (XRD). C-dots synthesized by this method were found to be exceptionally biocompatible against MDCK cells.

Liu *et al*., [339] synthesized high quantum yield carbon quantum dots (CQDs) via a green hydrothermal method using bamboo leaves. Branched polyethylenimine (BPEI)-capped CQDs (BPEI-CQDs) were prepared by coating the CQDs with BPEI via electrostatic adsorption; they were employed as fluorescent probes for sensitive and selective Cu^{2+} detection. Experimental results showed that the synthesized CQDs had an average diameter of 3.6 nm, with a narrow size distribution. The biomass-based CQDs offered a high quantum yield of 7.1%. The BPEI-CQDs-based sensing system rendered a simple, reliable, and sensitive Cu^{2+} detection with a detection limit as low as 115 nM and a dynamic range from 0.333 to 66.6 µM. In addition, the BPEI-CQDs were successfully used to detect Cu^{2+} in river water, demonstrating its excellent selectivity and great potential for analysis of environmental water samples.

Xu *et al*., [340] developed a green synthesis of water-soluble and well-dispersed fluorescent C-dots via a one-step hydrothermal treatment of potatoes. The as-prepared C-dots exhibited a strong blue fluorescence, with a quantum yield of up to 15%. They explored the use of these C-dots as a novel sensing probe for the label-free, sensitive, and selective detection of Fe^{3+} with the detection limit as low as 0.025 µmol L^{-1}, and different concentrations corresponding to different sensitivities [340].

A facile one-pot synthesis of fluorescent C-dots from orange waste peels has been developed via a hydrothermal carbonization method at a mild temperature (180 °C) [341]. The prepared hydrothermal carbons were amorphous in nature, and clusters of polyaromatic hydrocarbons included a large quantity of oxygen functional groups. A composite of C-dots with ZnO was used as a superior photocatalyst for the degradation of naphthol blue-black Azo dye under UV irradiation. In another study, Park *et al*., [342] developed a simple approach for the large-

scale synthesis of water-soluble green carbon nanodots (G-dots) from a variety of food waste-derived sources; ~ 120 grams of G-dots per 100 kilograms of food waste was synthesized using this simple and environment-friendly synthesis approach. The G-dots exhibited a high degree of solubility in water because of the abundant oxygen-containing functional groups on their surface. The narrow band of photoluminescence emission (approximately 400-470 nm) confirmed that the size of the G-dots was small (~ 4 nm) because of a similar quantum effect and emission trap on the surfaces. The G-dots had excellent photostability and their photoluminescence intensity slowly decreased (~8%) under continuous excitation with a Xe lamp for 10 days. A cell viability assay was conducted to assess the cytotoxicity effects of the G-dots on cells by introducing concentrations of G-dots, up to a 2 mg mL^{-1} for 24 h. The high photostability and low cytotoxicity exhibited by these G-dots renders them excellent probes for *in vitro* bio-imaging.

3.4. Exosome-like NPs

Communication between cells in multicellular organisms is an undeniable phenomenon. Exosomes are known to play a role in cell-cell communication and have, therefore, become a subject of increasing interest. Exosomes are nanosized microvesicles released from a variety of cells that can carry a cargo of proteins, lipids, mRNAs, and/or microRNAs, and transfer their cargo to recipient cells, thus, serving as extracellular messengers to mediate cell-cell communication. Recent investigations have suggested that nanosized particles from plant cells are exosome-like. In plants, exosomes derived from multivesicular bodies, may respond to plant pathogens as a means to regulate plant innate immunity. Ju *et al*.,[142] reported that the cells targeted by grape exosome-like NPs (GELNs) are intestinal stem cells, whose responses motivate GELN-mediated intestinal tissue remodeling and protection against dextran sulfate

sodium (DSS)-induced colitis. This finding is further supported by the fact that co-culturing of crypt or sorted $Lgr5^+$ stem cells with GELNs distinctly improved organoid formation. GELN lipids play a role in the induction of $Lgr5^+$ stem cells, and the liposome-like NPs assembled with lipids from GELNs are required for *in vivo* targeting of intestinal stem cells. Blocking β-catenin-mediated signaling pathways of GELN recipient cells attenuates the production of $Lgr5^+$ stem cells. Thus, GELNs not only modulate intestinal tissue renewal protocols, but can also participate in its remodeling in response to pathological triggers.

Wang *et al*.,[143] illustrated that grapefruit-derived nanovesicles (GDNs) were selectively taken up by intestinal macrophages and ameliorated DSS-induced mouse colitis. They demonstrated the development of GDNs for oral delivery of methotrexate to attenuate inflammatory responses in human disease. Furthermore, exosome-like NPs, isolated and characterized from four edible plants, were reported to contain proteins, lipids, and microRNA. The EPDENs were taken up by intestinal macrophages and stem cells, and the results generated from EPDEN-transfected macrophages indicated that ginger EPDENs preferentially induced the expression of the anti-oxidation gene, heme oxygenase-1, and the anti-inflammatory cytokine, IL-10; whereas, grapefruit, ginger, and carrot EPDENs promoted the activation of nuclear factors (erythroid-derived 2). Furthermore, analysis of the intestines of canonical Wnt-reporter mice revealed that the numbers of β-galactosidase$^+$ (β-Gal) intestinal crypts were increased, suggesting that EPDEN treatment of mice led to Wnt-mediated activation of the TCF4 transcription machinery in the crypts. These findings suggested a role for EPDEN-mediated interspecies communication by inducing expression of genes for anti-inflammation cytokines, anti-oxidation, and activation of Wnt signaling, which are crucial for maintaining intestinal homeostasis.

3.5. Adhesive NPs

Surface adhesion in nature is not an unknown phenomenon in the literature and several researchers have focused on this area over the past few years as they gear up to understand the chemical aspects of adhesion. While scientists have succeeded to determine some of the molecular structures present in the adhesives secreted by surface climbing or surface affixing biological systems, such as mussels and barnacles, the fundamental underlying adhesion mechanisms are still unknown (Figure 13).

Figure 13. Adhesive NPs - leaves of Sundew (left picture) are covered by small tentacles that generate the adhesive.

Studies have revealed that the natural biological systems utilize NPs to increase the surface adhesion [343]. Although, many advances have been made in the examination of micro- to nanoscale attachment mechanisms in animals, little attention has been paid to detection of similar phenomenon in plants. Lenaghan and Zhang [344] have explained that surfaces where ivy is attached had the presence of uniform NPs that were hypothesized to contribute to its amazing fastening strength. This persuasively illustrates that NPs are related to the adhesive forming

natural nanocomposite and highlights the importance of plant adhesion research for bio-inspiration to design strategies for novel nano-scale attachment. Huang *et al*., [145] concluded that the ivy NPs have the ability of preserving their UV protective capability in a wide range of temperature and pH values, thus offering a potential alternative to replace existing metal oxide NPs in sunscreen applications.

Xia *et al*., [144] examined the nanostructures formed by the soluble and insoluble parts of the sticky excretion from the mucilaginous rhizome of *Dioscorea opposita* and evaluated their cellular response. They found that the soluble extract of the excretion is able to shape a nanofibrillar scaffold made of uniform nanofibers, ~ 10 nm in size, with a typical pore size of ~ 40 nm, while nanofibers shaped by the insoluble extract did not have a specific structure. On the other hand, the nanofibrillar scaffold formed from the soluble extract provided an excellent platform for HeLa cell attachment and growth, and to a lesser degree for MC3T3 cells, while nanofibers from the insoluble extract revealed no cell attachment and growth. The nanofibrillar scaffold created from the *Dioscorea opposite* extract and its ability to sustain the attachment of specific cell types, demonstrated the potential for this natural nanomaterial in tissue engineering applications.

The diverse range of natural nanocomposites and their utility for tissue engineering has become an active topic in biomaterial research. Zhang *et al*., [345] investigated a nanofiber- and NP-based nanocomposite secreted from an insect-capturing plant, the Sundew, for cell attachment; the adhesive nanocomposite has a high biocompatibility and is ready for use with minimal preparation. Atomic force microscopy (AFM) examination of adhesive from three species of Sundew showed the existence of a nanofibers network and NPs, in various sizes. AFM

and light microscopy confirmed that a pattern of nanofibers corresponded to Alcian Blue staining for polysaccharides. TEM identified a low abundance of NPs in different patterns after AFM observations. Furthermore, the presence of Ca, Mg, and Cl (common components of biological salts) was revealed by EDS. Assessment of the material features of the adhesive showed a high viscoelasticity from the liquid adhesive, with reduced elasticity observed in the dried adhesive. At the same time, they illustrated that the ability of PC_{12} neuron-like cells to attach and grow on the network of nanofibers, created from the dried adhesive, can be useful in tissue engineering and other biomedical applications.

Yunnan baiyao, a traditional Chinese herbal medicine that has been used to treat wounds for centuries, was examined via AFM by Lenaghan *et al*. [346] which revealed the presence of uniform nanofibers in relatively high abundance in solution form; fibers were typically 25.1 nm in diameter and ranged in length from 86-726 nm. The unique structural and adhesive properties of nanofibers may play a vital role in platelet aggregation, leading to clotting, and the sealing of wounds.

3.6. Silica NPs

Elemental silicon has a wide range of traditional applications in metallurgy and in the semiconductor industry [146]. Nanostructured silicon materials are promising for a range of new technologies, such as nanoelectronics, photonics, biotechnology, energy harvesting, and energy storage (Figure 14). Silica NPs have varied and significant applications and can be produced in several forms, including fumed silica, colloidal silica, silica gel, and silica aerogel. Among the available agricultural bio-resources, rice husk is considered to be a cost-effective and non-metallic bio-precursor for synthesizing biogenic silica NPs.
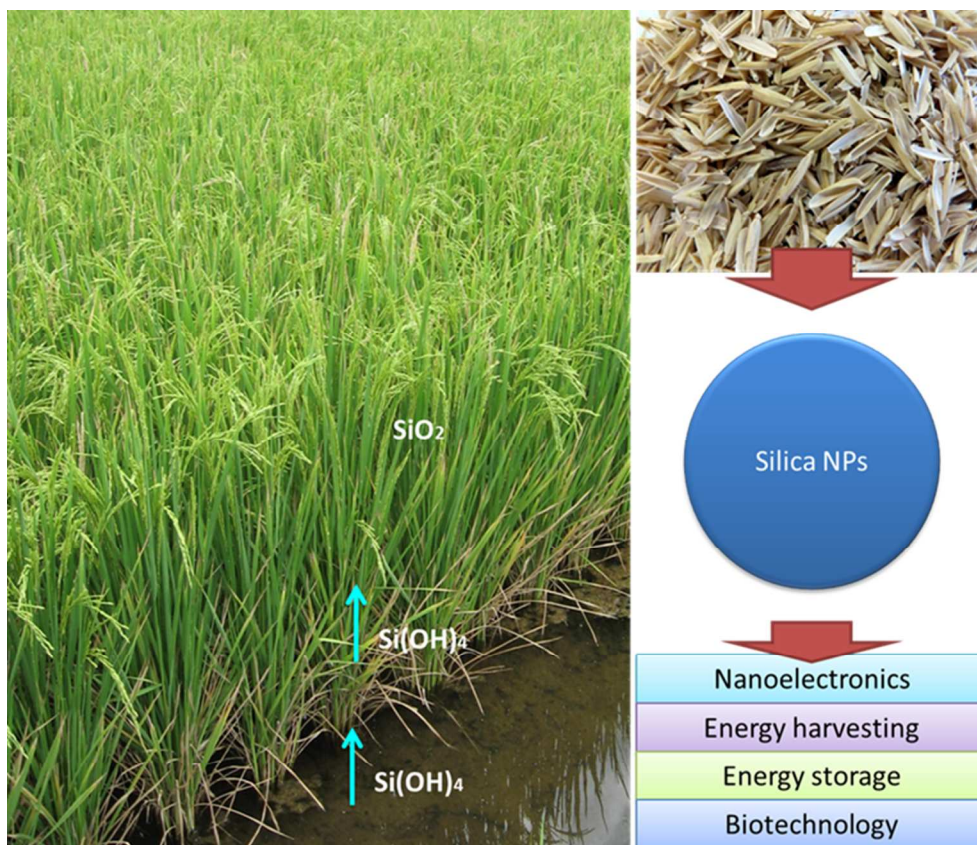
Figure 14. Silica NPs and their potential applications.

Rice (*Oryza sativa*) is the second-largest produced crop species worldwide (7.0×10^8 metric tons/year). Rice husks (RHs) and sugarcane bagasse are two of the highest-volume agricultural process residues. For every five tons of rice harvested, one ton of husk is produced, amounting to 1.2×10^8 tons of RHs per year across the globe. This enormous amount of waste by-product is an environmental nuisance and developing uses for these waste resources is associated with the global shift toward sustainable method development. However, current applications for the RHs have been limited to those with low added value, such as fertilizer additives, fuels, and land-fill or paving materials. The discovery pertaining to the recovery of high-value materials from RHs is desirable. RHs burn in air to form rice husk ash, and in this

process, the organic matter decomposes offering silica as the major remnant. Surprisingly, silica obtained in this manner is relatively pure and accounts for as much as approximately 20% of the dry weight of the RHs. Moreover, the silica within the RHs naturally exists in the form of NPs. As a living plant, rice absorbs silica in the form of silicic acid from soil, and the silica accumulates around cellulose micro-compartments. Therefore, RHs are a natural reservoir for nanostructured silica and its derivatives [146] (Figure 15).
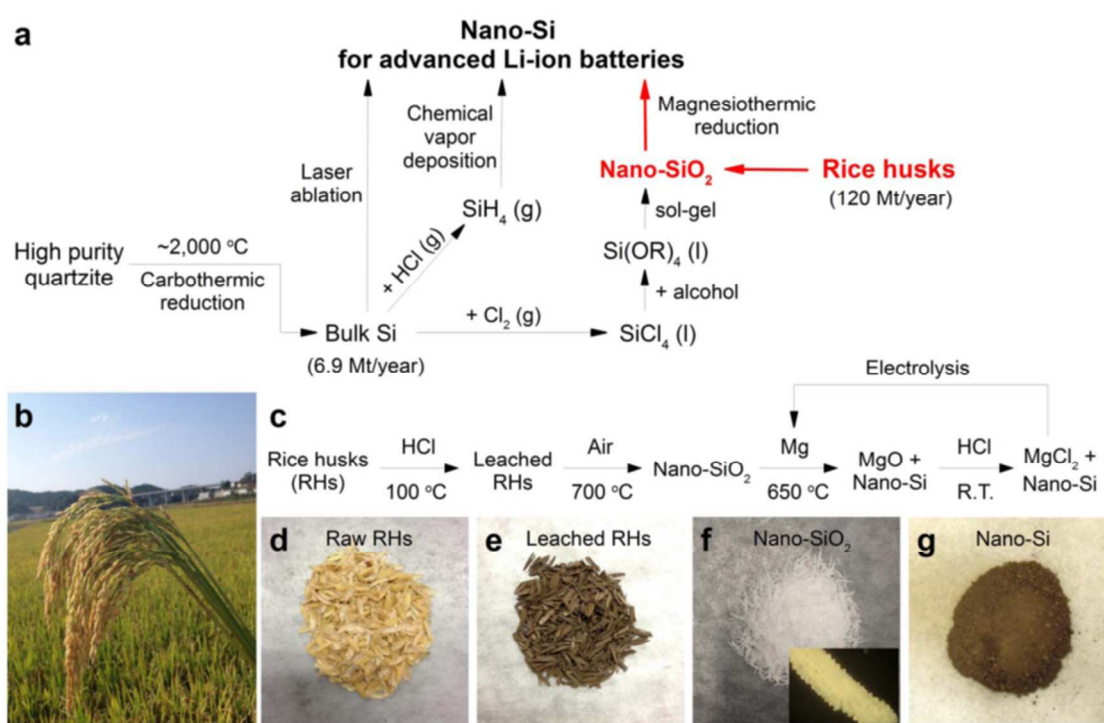
Figure 15. (a) A possibly low-cost, energy-efficient, green, and large scale production of nano-Si from RHs. Methods for producing nano-Si. Si(OR)$_4$ denotes silicon alkoxide. (b) A panicle of ripe rice at a rice farm in China (photographed by Huo, K.). (c) Flow chart of the process for recovering SiNPs from RHs. R.T. denotes room temperature. d–g, Optical images of the intermediate substances. The inset of (f) shows an optical microscopy image (0.9 mm 3 0.6 mm) of one piece of heat treated RH. Reproduced with permission from ref [347].

Athinarayanan *et al.,* [128] synthesized irregular biogenic silica NPs (approximately 10-30 nm) using rice husk as a precursor under pressurized conditions; the acid pretreatment of rice husk helps remove the inorganic impurities and induce the hydrolysis of organic substances. Residues from the acid pretreatment are calcinated at different temperatures for one hour; produced biogenic silica NPs can be used in bone tissue engineering [128].

Biogenic silica NPs (~25-30 nm) have been synthesized from RHs[348] and their characterization revealed that they comprise of smaller primary particles (~4.2 nm in diameter), and their clustering led to a porous structure with a surface area of 164 m^2/g. Under controlled-melting conditions catalyzed by K^+, these silica NP clusters gradually fused to form semi-crystalline porous silica frameworks with tunable pore size and structural integrity. Chen *et al.,* [349] have developed an approach for comprehensive utilization of RHs to obtain both lignocellulose and high quality porous silica NPs from RHs; most of the lignocellulose in RHs was first extracted by dissolution in ionic liquids, and subsequently separated and collected. The remaining RH residue following extraction, containing a high concentration of silica, was thermally treated to synthesize amorphous porous silica NPs with a high purity and surface area. It was found that during the extraction of lignocellulose using ionic liquids, some metal cations (*e.g.,* K^+) which generated a negative effect for the synthesis of silica, could be removed simultaneously thus generating a synergy for this comprehensive approach to make complete utilization of the RH biomass.

Liu *et al.,* [146] reported that pure silica NPs could be derived directly from RHs, an abundant agricultural byproduct produced at a rate of 1.2 × 108 tons/year, with a conversion yield as high as 5% by mass. Because of their small size (~ 10-40 nm) and porous nature, these

recovered silica NPs exhibited high performance as Li-ion battery anodes, with high reversible capacity (2,790 mA h g^{-1}, seven times greater than graphite anodes) and long cycle life (86% capacity retention over 300 cycles). Similarly, Xing *et al*., [350] demonstrated a scalable synthetic approach for the transformation of RH into highly valuable porous silicon using a magnesiothermic reaction; synthesized porous silicon, with a high porosity (0.62 cm^3 g^{-1}) and a large specific surface area (150.1 m^2 g^{-1}), is a promising material for lithium-ion battery applications. As an anode material, the porous silicon retained a considerably high reversible capacity of 1220.2 mA h g^{-1} at a specific discharge charge current of 1000 mA g^{-1} after 100 cycles.

Silica NPs from RH ash have been synthesized at room temperature using a high-energy planetary ball mill; the spherical nano-sized amorphous silica particles were formed after about 6 h of ball milling[351] and the average particle size was approximately 70 nm, which decreased with increasing ball milling time or mill's rotational speed. The as-synthesized silica NPs were subsequently employed as drug carriers for *in vitro* release behavior of Penicillin-G in simulated body fluid. Furthermore, Espíndola-Gonzalez *et al*., [147] reported the synthesis of silica oxide NPs from RH, sugar cane bagasse, and coffee husk, by employing vermicompost with annelids (*Eisenia foetida*); the generated product (humus) was calcinated and extracted to recover the crystalline NPs.

3.7. Lipids-based NPs

3.7.1. Cardanol

Cashew nut shell liquid (CNSL) is considered as an important starting material due to its abundant availability, low cost, and unique structural features (Figure 16). Several chemicals and products have been developed starting from CNSL by exploitingcthe three reactive sites, namely, unsaturation(s) in the alkenyl side chain, phenolic hydroxyl, and the aromatic ring [148].
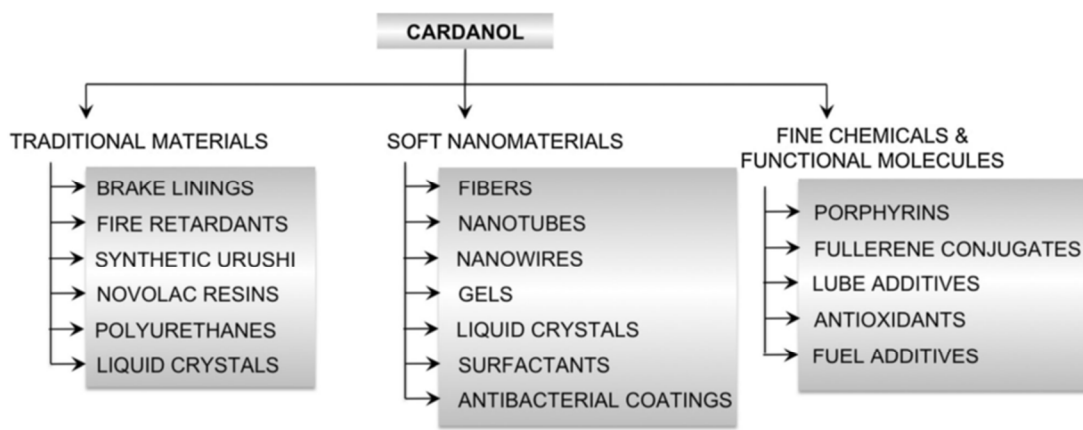
Figure 16. Cardanol as a renewable resource for diverse applications Reproduced from ref with permission from the Royal Society of Chemistry [149].

Cardanol, a biobased lipid-mixture obtained from the plant *Anacardium occidentale* L., is a renewable raw material derived from a byproduct of cashew nut processing industry. This bio-based lipid-mixture is a rich mixture of non-isoprenoic phenolic compounds, which is a valuable raw material for generating several soft nanomaterials such as nanofibers, nanotubes, gels and surfactants which may then serve as templates for the synthesis of additional nanomaterials [149] (Figure 17).

Glylip-1 = (a+b+c+d); Glylip-2 = d
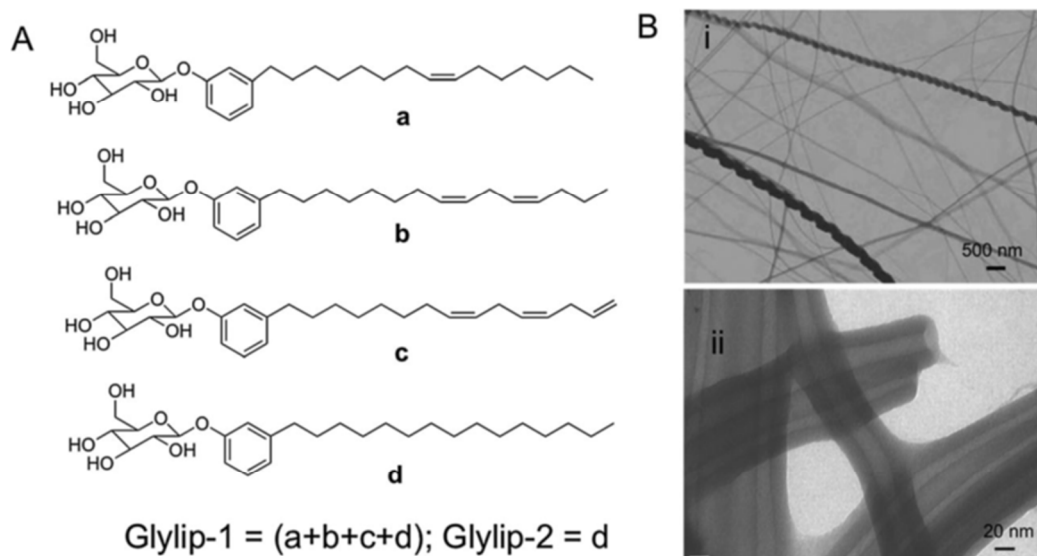
Figure 17. (A) Chemical structures of cardanol glycolipids, and (B) their self-assembly to form (i) helical fibers and (ii) nanotubes. Reproduced from ref [149] with permission from the Royal Society of Chemistry.

4. Challenges and future scope

The use of plants in green nanotechnology and nanobiotechnology is developing rapidly and plant-derived nanostructures have found numerous applications in diverse fields including photocatalysis, solar cell devices, biosensors, catalysis, biomedicine, electronics, sensing, photonics, environmental clean-up, imaging, bio-labeling, drug and gene delivery, and biomaterials. The non-toxic and biocompatible properties of these nanostructures enable their applications in biomedical sciences such as tissue engineering as well as in pharmaceutical industries [347, 352-356].

There has been a huge surge of interest in the use of biomass as a renewable source of energy and materials; cellulose, as a nanostructured material in the form of nanocellulose is one, among others. Chemically, it mainly consists of cellulose nanocrystals or mechanically extracted

NPs (micro-fibrillated cellulose). On this related theme, several explorations have been conducted for the production of plant-derived nanostructures on a large scale exemplified in the production of starch nanocrystals, curcumin NPs and other nanocellulose-based materials. The ongoing investigations in this area would promote the development of greener methods to generate nanostructures of various shapes and sizes, from renewable and biodegradable precursor chemicals, thus precluding the use of hazardous organic solvents, and associated by-products, which often raise environmental concerns. Although there is a significant benefit in developing nontoxic, inexpensive, and eco-friendly processes in this context, but several important challenges and technical problems need to be circumvented. As an example, in phyto-formulation studies, researchers have focused their attention on developing nano dosage forms, including liposomes, proliposomes, solid lipid NPs, nano-emulsions, and protein-based and lipid-based drug delivery systems etc. In this domain, bioavailability, the enhancement of solubility and toxicity prevention, enhancement of pharmacological activity and stability, improving tissue macrophages distribution, sustained delivery, and avoidance of physical and chemical degradation are some of the important prerequisites. It is crucial to discuss the issue of large-scale production of nanostructures which governs their practical applications as commercial products.

4. Conclusion

Development of biomimetic and bio-inspired approaches to nanostructures is one of the most promising scientific and technological challenges in the coming years for the development of advanced technologies, namely bio-inspired materials and systems, adaptive materials, hierarchically structured materials, 3D composites, and nanomaterials that are compatible with

ecological requirements. Bio-inspired and selective multi-functional materials, with associated applications (such as separation, adsorption, catalysis, imaging, biosensing, sensing, and multi-therapy), will undoubtedly be emphasized in future research endeavors for the sustainable use of renewable resources. Greener nanofabrication has been actively pursued in recent years to meet the need for large quantities of highly purified, structurally well-defined, and precisely functionalized nanomaterials. In the present review, an overview of natural nanomaterials originating from live plants or plant-derived materials, and a discussion of their potential applications in diverse disciplines including biomedical applications is presented. Despite the progress achieved to date, considerable challenges exist that must be addressed to obtain optimal performance and derive maximum benefits from the complete and exhaustive use of these plant-based green nano-manufacturing systems.

Disclaimer

U.S. Environmental Protection Agency (EPA), through its Office of Research and Development, partially funded and collaborated in, the research described herein. It has been subjected to the Agency's administrative review and has been approved for external publication. Any opinions expressed in this paper are those of the author(s) and do not necessarily reflect the views of the Agency, therefore, no official endorsement should be inferred. Any mention of trade names or commercial products does not constitute endorsement or recommendation for use.

List of abbreviations

Atomic Force Microscopy…………………………………………..AFM

Branched Polyethyleneamine-capped Carbon Quantum Dots………..BPEI-CQDs

Cashew Nut Shell Liquid…………………………………………...CNSL

79

Nanoparticles………………………………………………………..… NPs

Palladium…………………………………………………….…………Pd

Phosphate Buffered Saline……………………………………......…..PBS

Polymerase Chain Reaction…………………………………......….. PCR

Quantum Yield………………………………………………...….……QY

Retinoic Acid……………………………………………….…..…… RA

Rice Husks…………………………………………………………..RHs

Scanning Electron Microscopy……………………………….….…SEM

Single-wall Nanotubes………………………………………...…… SWNT

Soy Protein Isolate…………………………………………….. SPI

2,2,6,6-tetramethylpi-peridine-1-oxyl………………………………..TEMPO

Three-Dimensional……………………………………………....…3D

α-Tocopherol……………………………………………….…..TOC

Transmission Electron Microscopy………………………………..... TEM

Ultra Violet……………………………………………………….. UV

Vapor-liquid-solid……………………………………………….VLS

Vitamin D3……………………………………………………..…..VD3

Water-soluble Carbon Nano-onions………………………………….… wsCNOs

X-ray Diffraction………………………………………………..XRD

Zein/Ibuprofen……………………………………………..……..IBU

Zein NPs……………………………………………….....……..ZN

Biographies

Reza Mohammadinejad was born in Sirjan, Iran (1987). He received his B.S. in Plant Pathology from Vali-e-Asr University of Rafsanjan (2009) and M.S. in Agricultural Biotechnology from Graduate University of Advanced Technology (2013). Recently, he is engaged in the synthesis of nanoparticles from mineral waste and their applications for water desalination. His research interests include nanobiotechnology, bio-inspired nanotechnology and bioengineering.

Samaneh Karimi received her PhD in bio-nanocomposite technology, in 2014 from the Institute of Tropical Forestry and Forest Products, University Putra Malaysia. Presently, she is a scientist at the Plant and Food Research Institute in Lincoln, New Zealand. Her main research interests

relate to the processing and characterization of bio-based polymeric nanofibers through a variety of techniques and their applications in diverse fields, e.g. biomedical engineering and nanocomposites.

Siavash Iravani was born in Iran (Pharm.D., Ph.D.). He has worked on several projects at the Isfahan University of Medical Sciences (Faculty of Pharmacy and Pharmaceutical Sciences), including green and eco-friendly synthesis of nanomaterials, phytochemical analysis of pine bark extracts, technological and stability aspects of probiotic fermented milks, gene delivery systems for prostate cancer therapy, nanoparticles for drug delivery in cancer, nano carriers, and drug nanoparticles. His previous experience, for more than 5 years, centers on drug development and industrial pharmacy in various capacities including research and development, formulation, and quality control. Dr. Iravani has authored over 30 peer-reviewed publications and five book chapters.

Rajender S. Varma was born in India (Ph.D., Delhi University 1976). After postdoctoral research at Robert Robinson Laboratories, Liverpool, U.K., he was a faculty member at Baylor College of Medicine and Sam Houston State University prior to joining the Sustainable Technology Division at the US Environmental Protection Agency in 1999. He has over 40 years of research experience in management of multidisciplinary technical programs ranging from natural products chemistry to development of more environmentally friendly synthetic methods using microwaves, ultrasound, etc. Lately, he is focused on greener approaches to assembly of nanomaterials and the sustainable applications of magnetically retrievable nanocatalysts in benign media. He is a member of the editorial advisory board of several international journals, has published over 420 scientific papers, and has been awarded 14 US Patents.

References

1.   A. Hoffman, G. Mills, H. Yee and M. Hoffmann, *The Journal of Physical Chemistry*, 1992, **96**, 5546-5552.

2.   G. Schmid, *Chemical Reviews*, 1992, **92**, 1709-1727.

3.   V. Colvin, M. Schlamp and A. Alivisatos, *Nature*, 1994, **370**, 354-357.

4.   Y. Wang and N. Herron, *The Journal of Physical Chemistry*, 1991, **95**, 525-532.

5.   H. S. Mansur, F. Grieser, M. S. Marychurch, S. Biggs, R. S. Urquhart and D. N. Furlong, *Journal of the Chemical Society, Faraday Transactions*, 1995, **91**, 665-672.

6.   Y. Wang, *Accounts of chemical research*, 1991, **24**, 133-139.

7.   A. Yoffe, *Advances in Physics*, 1993, **42**, 173-262.

8.   M. M. Azmi, Z. Tehrani, R. Lewis, K.-A. Walker, D. Jones, D. Daniels, S. Doak and O. Guy, *Biosensors and Bioelectronics*, 2014, **52**, 216-224.

9.   D. Pan, L. Mi, Q. Huang, J. Hu and C. Fan, *Integrative Biology*, 2012, **4**, 1155-1163.

10.   J. Yao, M. Yang and Y. Duan, *Chemical reviews*, 2014, **114**, 6130-6178.

11.   J. Virkutyte and R. S. Varma, *Chem. Sci*, 2011, **2**, 837-846.

12.   S. Shukla, C. Dickmeis, A. Nagarajan, R. Fischer, U. Commandeur and N. Steinmetz, *Biomaterials Science*, 2014, **2**, 784-797.

13.   A. Kumar and V. Kumar, *Chemical reviews*, 2014, **114**, 7044-7078.

14.   K. Ashtari, J. Fasihi, N. Mollania and K. Khajeh, *Materials Research Bulletin*, 2014, **50**, 348-353.

15.   S. S. Behrens, *Encyclopedia of Inorganic and Bioinorganic Chemistry*, Wiley, 2013.

16.   K. Cung, B. J. Han, T. D. Nguyen, S. Mao, Y.-W. Yeh, S. Xu, R. R. Naik, G. Poirier, N. Yao and P. K. Purohit, *Nano letters*, 2013, **13**, 6197-6202.

17.   L. Gao and N. Ma, *ACS nano*, 2011, **6**, 689-695.

18.   W. Gao, X. Feng, A. Pei, C. R. Kane, R. Tam, C. Hennessy and J. Wang, *Nano letters*, 2013, **14**, 305-310.

19.   A. Kumar and B. Singh, *RSC Advances*, 2012, **2**, 9079-9090.

20.   Z. Tong, Y. Jiang, D. Yang, J. Shi, S. Zhang, C. Liu and Z. Jiang, *RSC Advances*, 2014, **4**, 12388-12403.

21.   R. Govaerts, *Taxon*, 2001, 1085-1090.

22.   S. Iravani, *Green Chem.*, 2011, **13**, 2638-2650.

23.   S. Iravani, H. Korbekandi, S.V. Mirmohammadi and B. Zolfaghari, *Research in Pharmaceutical Sci.*, 2014, **9**, 385-406.

24.   S. Iravani and B. Zolfaghari, *Biomed Research International*, 2013, 2013, 10.1155/2013/639725, 5.

25.   H. Korbekandi, Z. Ashari, S. Iravani and S. Abbasi., *Iranian journal of pharmaceutical research*, 2013, **12**, 289-298.

26.   H. Korbekandi and S. Iravani, in *Green biosynthesis of nanoparticles: mechanisms and applications* eds. Rai M and C. Posten, CABI, Wallingford, UK, 2013, pp. 53-60.

27.   H. Korbekandi, S. Iravani and S. Abbasi, *Critical Reviews in Biotechnology*, 2009, **29**, 279-306.

28.   H. Korbekandi, S. Iravani and S. Abbasi, *Journal of Chemical Technology & Biotechnology*, 2012, **87**, 932-937.

29.   M. N. Nadagouda, A. B. Castle, R. C. Murdock, S. M. Hussain and R. S. Varma, *Green Chem.*, 2010, **12**, 114-122.

30.   M. N. Nadagouda, V. Polshettiwar and R. S. Varma, *J. Mater. Chem*, 2009, **19**, 2026-2031.

31.   M. N. Nadagouda, T. F. Speth and R. S. Varma, *Acc. Chem. Res*, 2011, **44**, 469-478.

32.   M. N. Nadagouda and R. S. Varma, *Green Chem*, 2008, **10**, 859-862.

33.   M. N. Nadagouda and R. S. Varma, *J. Nanomater*, 2008, **10**.1155/2008/782358.

34.   A. Baghizadeh, S. Ranjbar, V. K. Gupta, M. Asif, S. Pourseyedi, M. J. Karimi and R. Mohammadinejad, *Journal of Molecular Liquids*, 2015, **207**, 159-163.

35.   A. K. Mittal, Y. Chisti and U. C. Banerjee, *Biotechnology advances*, 2013, **31**, 346-356.

36.   R. Mohammadinejad, S. Pourseyedi, A. Baghizadeh, S. Ranjbar and G. Mansoori, Int. J. Nanosci. Nanotechnol. 2013, 9, 221-226.37. K.B.A. Ahmed, S. Subramanian, A. Sivasubramanian, G. Veerappan and A. Veerappan, *Spectrochimica Acta Part A: Molecular and Biomolecular Spectroscopy*, 2014, **130**, 54-58.

38.   A. Gade, S. Gaikwad, N. Duran and M. Rai, *Micron*, 2014, **59**, 52-59.

39.   M. Khan, M. Khan, M. Kuniyil, S.F. Adil, A. Al-Warthan, A. HZ and et. al, *Dalton Transactions*, 2014, 10.1039/C3DT53554A.

40.   D.A. Kumar, V. Palanichamy and S. Roopan, *Spectrochimica Acta Part A: Molecular and Biomolecular Spectroscopy*, 2014, **127**, 168-171.

41.   R. Mariselvam, A.J.A. Ranjitsingh, A. Usha Raja Nanthini, K. Kalirajan, C. Padmalatha and P.-M. Selvakumar, *Spectrochimica Acta Part A: Molecular and Biomolecular Spectroscopy*, 2014, **129**, 537-541.

42.   C.K. Sathiya and S. Akilandeswari, *Spectrochimica Acta Part A: Molecular and Biomolecular Spectroscopy*, 2014, **128**, 337-341.

43.   Q. Sun, X. Caia, J .Li, M. Zheng, Z. Chen and C.-P. Yu, *Colloids and Surfaces A: Physicochem. Eng. Aspects*, 2014, **444**, 226-231.

44.   G. Suresh, P.H. Gunasekar, D. Kokila, D. Prabhu, D. Dinesh, N. Ravichandran and et. al, *Spectrochimica Acta Part A: Molecular and Biomolecular Spectroscopy*, 2014, **127**, 61-66.

45.   P. Velmurugan, K. Anbalagan, M. Manosathyadevan, K.J. Lee, M. Cho, S.M. Lee and et. al, *Bioprocess and Biosystems Engineering*, 2014, 10.1007/s00449-014-1169-6.

46.   S.R. Vijayan, P. Santhiyagu, M. Singamuthu, N.K. Ahila, R. Jayaraman and K. Ethiraj, *The Scientific World Journal*, 2014, 2014, http://dx.doi.org/10.1155/2014/938272.

47.   K. Vimala, S. Sundarraj, M. Paulpandi, S. Vengatesan and S. Kannan, *Process Biochemistry*, 2014, **49**, 160–172.

48.   R. Yuvakkumar, J. Suresh, A. Joseph Nathanael, M. Sundrarajan and S.-I. Hong, *Materials Science and Engineering: C*, 2014, **41**, 17-27.

49.   C. Coman, L.F. Leopold, O.D. Rugină, L. Barbu-Tudoran, N. Leopold, M. Tofană and et. al, *Journal of Nanoparticle Research*, 2013, **16**, 2158.

50.   S. Gunalan, R. Sivaraj and R. Venckatesh, *Spectrochimica Acta Part A: Molecular and Biomolecular Spectroscopy*, 2012, **97**, 1140–1144.

51.   K.L. Niraimathi, V. Sudha, R. Lavanya and P. Brindha, *Colloids and Surfaces B: Biointerfaces*, 2013, **102**, 288- 291.

52.   S. Sulochana, P. Krishnamoorthy and K. Sivaranjani, *J Pharmacol Toxicol*, 2012, **7**, 251-258.

53.   S.M. Roopan, A. Bharathi, R. Kumar, V.G. Khanna and A. Prabhakarn, *Colloids and Surfaces B: Biointerfaces*, 2012, **92**, 209-212.

54.   A.J. Kora and J. Arunachala, *J Nanomater*, 2012, **2012**, doi:10.1155/2012/869765.

55.   S.S. Shankar, A. Rai, A. Ahmad and M. Sastry, *J Colloid Interf Sci*, 2004, **275**, 496-502.

56.   A. Thirumurugan, G.J. Jiflin, G. Rajagomathi, N.A. Tomy, S. Ramachandran and R. Jaiganesh, *Int J Biol Tech*, 2010, **1**, 75-77.

57.   S. Aswathy Aromal and D. Philip, *Physica E: Low-dimensional Systems and Nanostructures*, 2012, **44**, 1329-1334.

58.   S. Harne, A. Sharma, M. Dhaygude, S. Joglekar, K. Kodam and M. Hudlikar, *Colloids and Surfaces B: Biointerfaces*, 2012, **95**, 284-288.

59.   S.K. Boruah, P.K. Boruah, P. Sarma, C. Medhi and O.-K. Medhi, *Advanced Materials Letters*, 2012, **3**, 481-486.

60.   D. Jain, H.K. Daima, S. Kachhwaha and S.-L. Kothari, *Dig J Nanomater Bios*, 2009, **4**, 557- 563.

61.   N. Mude, A. Ingle , A. Gade and M. R, *Journal of Plant Biochemistry and Biotechnology*, 2009, **18**, 83-86.

62.   M. Sathishkumar, K. Sneha, Seob Kwak In, J. Mao, S.J. Tripathy and Y.S. Yun, *Journal of Hazardous Materials*, 2009, **171**, 400-404

63.   M. Sathishkumar, K. Sneha, S.W. Won, C.-W Cho, S. Kim and Y.S. Yun, *Colloids and Surfaces B: Biointerfaces*, 2009, **73**, 332-338.

64.   Y. Xin, L. Qingbiao, W. Huixuan, H. Jiale, L. Liqin, W. Wenta and et. al, *J Nanopart Res*, 2010, **12**, 1589-1598.

65.   K. Satyavani, T. Ramanathan and S. Gurudeeban, *J Nanosci Nanotechnol*, 2011, **1**, 95- 101.

66.   M. Vanaja and G. Annadurai, *Appl Nanosci*, 2012, doi.10.1007/s13204-012-0121-9.

67.   D. Gnanasangeetha and D. SaralaThambavani, *Research Journal of Material Sciences*, 2013, **1**, 1-8.

68.   A.K. Jha and K. Prasad, *International Journal of Green Nanotechnology: Physics and Chemistry*, 2010, **1**:2, 110-117.

69.   A.K. Jha, K. Prasad, K. Prasad and A. Kulkarni, *Colloids and Surfaces B: Biointerfaces*, 2009, **73**, 219-223.

70.   J. Kesharwani, K.Y. Yoon, J. Hwang and M. Rai, *Journal of Bionanoscience*, 2009, **3**, 1-6.

71.   N. Ahmad, S. Sharma, V.N. Singh, S.F. Shamsi, A. Fatma and B.R. Mehta, *Biotechnology Research International*, 2011, **2011**, doi:10.4061/2011/454090.

72.   J.Y. Song, E.Y. Kwon and B.S. Kim, *Bioprocess Biosyst Eng*, 2010, **33**, 159-164.

73.   S. Ghosh, S. Patil, M. Ahire, R. Kitture, S. Kale and K. Pardesi, *Int J Nanomed*, 2012, **7**, 483- 496.

74.   R.U. Maheswari, A.L. Prabha, V. Nandagopalan and V. Anburaja, *IOSR J Pharma Biol Sci*, 2012, **1**, 38- 42.

75.   G. Rajakumar, A.A. Rahuman, B. Priyamvada, V.G. Khanna, D.K. Kumar and P.-J. Sujin, *Materials letters*, 2012, **68**, 115–117.

76.   G. Gnanajobitha, G. Annadurai and C. Kannan, *Int J Pharma Sci Res*, 2012, **3**, 323-330.

77.   M. Dubey, S. Bhadauria and B. Kushwah, *Digest Journal of Nanomaterials and Biostructures*, 2009, **4**, 537-543.

78.   M. Valodkar, R.N. Jadeja, M.C. Thounaojam, R.V. Devkar and S. Thakore, *Materials Chemistry and Physics*, 2011, **128**, 83-89

79. L. Marchiol, A. Mattiello, F. Pošćić, C. Giordano and R. Musetti, *Nanoscale Research Letters*, 2014, **9**, 101.

80. L. Jia, Q. Zhang, Q. Li and H. Song, *Nanotech*, 2009, **20**, doi:10.1088/0957-4484/20/38/385601.

81. R.K. Petla, S. Vivekanandhan, M. Misra, A.K. Mohanty and N. Satyanarayana, *J. Biomater. Nanobiotechnol*, 2012, **3**, 14-19.

82. S. Dinesh, S. Karthikeyan and P. Arumugam, *Arch Appl Sci Res*, 2012, **4**, 178-187.

83. M.R. Bindhu and M. Umadevi, *Spectrochim Acta A Mol Biomol Spectrosc*, 2012, **101**, 184-190.

84. N. Sable, S. Gaikwad, S. Bonde, A. Gade and M.M. Rai, *Nus Biosci*, 2012, **4**, 45-49.

85. M.F. Fazaludeena, C. Manickamb, M.A.I. Ashankytyc, M.Q. Ahmedd and Z.B. Quaser, *J. Microbiol Biotech Res*, 2012, **2**, 23-34.

86. P. Sivakumar, C. Nethradevi and S. Renganathan, *Asian J Pharm Clin Res*, 2012, **5**, 97-101.

87. A.-R Im, L. Han, E.R. Kim, J. Kim, Y.S. Kim and Y. Park, *Phytother Res*, 2012, **26**, 1249-1255.

88. J.Y. Song, H.-K Jang and B. Kim, *Process Biochemistry*, 2009, **44**, 1133–1138.

89. D.M. Ali, N. Thajuddin, K. Jeganathan and M. Gunasekaran, *Colloids Surf B Biointerfaces*, 2011, **85**, 360-365.

90. P.S. Vankar and D. Bajpai, *Indian J Biochem Biophys*, 2010, **47**, 157- 160.

91. M. EJ and L. Inbathamizh, *Asian J Pharm Clin Res*, 2012, **5**, 159-162.

92. C. Soundarrajan, A. Sankari, P. Dhandapani, S. Maruthamuthu, S. Ravichandran, G. Sozhan and N. Palaniswamy, *Bioprocess Biosyst Eng*, 2012, **35**, 827-833.

93.   C. Ramteke, T. Chakrabarti, B.K. Sarangi and R. Pandey, *J Chem*, 2013, **2013**,
        doi.org/10.1155/2013/278925.

94.   V. Vignesh, K.F. Anbarasi, S. Karthikeyeni, G. Sathiyanarayanan, P. Subramanian and R.
        Thirumurugan, *Colloids and Surfaces A: Physicochemical and Engineering Aspects*,
        2013, **439**, 184–192.

95.   D. A. Kumar, *Int Res J Pharma*, 2012, **3**, 169-173.

96.   C. Sundaravadivelan and M. Nalini, *Asian Pac J Trop Biomed*, 2011, **2012**, 1-8.

97.   S.S. Shankar, A. Absar and S. Murali, *Biotechnol Prog*, 2003, **19**, 1627-1631.

98.   F. Coccia, L. Tonucci, D. Bosco, M. Bressan and N.-D. Alessandro, *Green Chem*, 2012,
        14, 1073-1078.

99.   K. Mallikarjuna, G.R. Dillip, G. Narashima, N.J. Sushma and B.D.P. Raju, *Res J Nanosci
        Nanotech*, 2012, **2**, 17-23.

100.   K. Mallikarjuna, N. John Sushma, B.V. Subba Reddy, G. Narasimha and B. D. P. Raju,
        International Journal of Chemical and Analytical Science, 2013, **4**, 14-18.

101.   S. Garg, *Int J Innov Biol Chem Sci*, 2012, **3**, 5-10.

102.   D.C. Patil, V.S. Patil, P.H. Borase, K.B. Salunke and B.R. Salunkhe, *Parasitol Res*, 2012,
        110, 1815-1822.

103.   S.S. Dash, R. Majumdar, A.K. Sikder, B.G. Bag and B.-K. Patra, *Appl Nanosci*, 2014, **4**,
        485–490.

104.   A. Nabikhan, K. Kandasamy, A. Raj and N.M. Alikunhi, *Colloids and Surfaces B:
        Biointerfaces*, 2010, **79**, 488–493.

105.   M.R. Bindhu and M. Umadevi, *Spectrochimica Acta Part A: Molecular and
        Biomolecular Spectroscopy*, 2014, **128**, 37–45.

106.　M. Amin, F. Anwar, M.R.S.A. Janjua, M.A. Iqbal and U. Rashid, *Int J Mol Sci*, 2012, **13**, 9923- 9941.

107.　E.C. Njagi, H. Huang, L. Stafford, H. Genuino, H.M. Galindo, J.B. Collins and et. al, *Langmuir*, 2011, **27**, 264-271.

108.　R. Deshpande, M.D. Bedre, S. Basavaraja, B. Sawle, S.Y. Manjunath and A. Venkataraman, *Colloids and Surfaces B: Biointerfaces*, 2010, **79**, 235-240.

109.　S. Yallappa, J. Manjanna, M.A. Sindhe, N.D. Satyanarayan, S.N. Pramod and K. Nagaraja, *Spectrochimica Acta Part A: Molecular and Biomolecular Spectroscopy*, 2013, **110**, 108-115.

110.　B. Ankamwar, *E-Journal of Chemistry*, 2010, **7**, 1334-1339.

111.　K.M. Kumar, M. Sinha, B.K. Mandal, A.R. Ghosh, K.S. Kumar and P.S. Reddy, *Spectrochimica Acta Part A*, 2012, **91**, 228-233.

112.　R. Geethalakshmi and D.V.L. Sarada, *Int J Eng Sci Technol*, 2010, **2**, 970- 975.

113.　K. Gopalakrishnan, C. Ramesh, V. Ragunathan and M. Thamilselvan, *Dig J Nanomater Bios*, 2012, **7**, 833-839.

114.　C. Singh, V. Sharma, K.R.P. Naik, V. Khandelwal and H. Singh, *Dig J Nanomater Bios*, 2011, **6**, 535-542.

115.　M. Rai and A. Ingle, *Applied microbiology and biotechnology*, 2012, **94**, 287-293.

116.　M. Naderi and A. Danesh-Shahraki, *International Journal of Agriculture and Crop Sciences*, 2013, **5**, 2229-2232.

117.　S. Joseph, E. Graber, C. Chia, P. Munroe, S. Donne, T. Thomas, S. Nielsen, C. Marjo, H. Rutlidge and G. Pan, *Carbon Management*, 2013, **4**, 323-343.

118. F. Torney, B.G. Trewyn, V.S.Y. Lin and K. Wang, *Nature Nanotechnology*, 2007, **2**, 295-300.

119. M. V. Khodakovskaya, K. de Silva, A. S. Biris, E. Dervishi and H. Villagarcia, *ACS nano*, 2012, **6**, 2128-2135.

120. J. P. Giraldo, M. P. Landry, S. M. Faltermeier, T. P. McNicholas, N. M. Iverson, A. A. Boghossian, N. F. Reuel, A. J. Hilmer, F. Sen and J. A. Brew, *Nature materials*, 2014, **13**, 400-408.

121. S. Chandra, S. Pradhan, S. Mitra, P. Patra, A. Bhattacharya, P. Pramanik and A. Goswami, *Nanoscale*, 2014, **6**, 3647-3655.

122. S. Yi, Y. Wang, Y. Huang, L. Xia, L. Sun, S. C. Lenaghan and M. Zhang, *Journal of biomedical nanotechnology*, 2014, **10**, 1016-1029.

123. S. Daus and T. Heinze, *Macromol Biosci*, 2010, **10**, 211-220.

124. M.-L. Kung, P.-Y. Lin, C.-W. Hsieh, M.-H. Tai, D.-C. Wu, C.-H. Kuo, S.-L. Hsieh, H.-T. Chen and S. Hsieh, *ACS Sustainable Chemistry & Engineering*, 2014, **2**, 1769-1775.

125. A. Johnson-Buck, G. Kim, S. Wang, H. J. Hah and R. Kopelman, *Molecular Crystals and Liquid Crystals*, 2009, **501**, 138-144.

126. H. Koga, M. Nogi, N. Komoda, T. T. Nge, T. Sugahara and K. Suganuma, *NPG Asia Materials*, 2014, **6**, e93.

127. I. Gilca, V.I. Popa and C. Crestini, *Ultrason Sonochem*, 2015, 369-375.

128. J. Athinarayanan, V. S. Periasamy, M. Alhazmi, K. A. Alatiah and A. A. Alshatwi, *Ceramics International*, 2015, **41**, 275-281.

129. V. N. Mehta, S. Jha and S. K. Kailasa, *Materials Science and Engineering: C*, 2014, **38**, 20-27.

130.   H. Yuan, D. Li, Y. Liu, X. Xu and C. Xiong, *Analyst*, 2015.

131.   N. Reddy, Z. Shi, H. Xu and Y. Yang, *J Biomed Mater Res A*, 2015, **103**, 1653-1658.

132.   E.-P Ng, H. Awala, K.-H Tan, F. Adam, R. Retoux and S. Mintov, *Microporous and Mesoporous Materials*, 2015, **204**, 204–209.

133.   D. Whitford, *Proteins: structure and function*, John Wiley & Sons, 2013.

134.   H. Xu, Q. Jiang, N. Reddy and Y. Yang, *Journal of Materials Chemistry*, 2011, **21**, 18227-18235.

135.   N. Lin and A. Dufresne, *European Polymer Journal*, 2014, **59**, 302-325.

136.   S. Karimi, P. M. Tahir, A. Karimi, A. Dufresne and A. Abdulkhani, *Carbohydrate polymers*, 2014, **101**, 878-885.

137.   L. Berglund, CRC Press: Boca Raton, FL, 2005.

138.   E. T. Mickelson, Ph. D. Thesis, Rice University, Houston, TX, 1999.

139.   H. Muramatsu, Y. A. Kim, K. S. Yang, R. Cruz-Silva, I. Toda, T. Yamada, M. Terrones, M. Endo, T. Hayashi and H. Saitoh, *Small*, 2014, **10**, 2766-2770.

140.   X.-W. Chen, O. Timpe, S. B. Hamid, R. Schlögl and D. S. Su, *Carbon*, 2009, **47**, 340-343.

141.   J. Zhu, J. Jia, F. L. Kwong, D. H. L. Ng and S. C. Tjong, *biomass and bioenergy*, 2012, **36**, 12-19.

142.   S. Ju, J. Mu, T. Dokland, X. Zhuang, Q. Wang, H. Jiang, X. Xiang, Z.-B. Deng, B. Wang and L. Zhang, *Molecular Therapy*, 2013, **21**, 1345-1357.

143.   B. Wang, X. Zhuang, Z.-B. Deng, H. Jiang, J. Mu, Q. Wang, X. Xiang, H. Guo, L. Zhang and G. Dryden, *Molecular Therapy*, 2014, **22**, 522-534.

144.   L. Xia, S. C. Lenaghan, A. B. Wills, Y. Chen and M. Zhang, *Colloids and Surfaces B: Biointerfaces*, 2011, **88**, 425-431.

145.   Y. Huang, S. C. Lenaghan, L. Xia, J. N. Burris, C. N. Stewart Jr and M. Zhang, *Journal of nanobiotechnology*, 2013, **11**.

146.   N. Liu, K. Huo, M. T. McDowell, J. Zhao and Y. Cui, *Scientific reports*, 2013, **3**.

147.   A. Espíndola-Gonzalez, A. Martínez-Hernández, C. Angeles-Chávez, V. Castano and C. Velasco-Santos, *Nanoscale research letters*, 2010, **5**, 1408-1417.

148.   C. Voirin, S. Caillol, N. V. Sadavarte, B. V. Tawade, B. Boutevin and P. P. Wadgaonkar, *Polymer Chemistry*, 2014, **5**, 3142-3162.

149.   V. S. Balachandran, S. R. Jadhav, P. K. Vemula and G. John, *Chemical Society Reviews*, 2013, **42**, 427-438.

150.   A.-M. Orecchioni, C. Duclairoir, D. Renard and E. Nakache, *Journal of nanoscience and nanotechnology*, 2006, **6**, 3171-3178.

151.   N. Reddy and Y. Yang, *Trends in biotechnology*, 2011, **29**, 490-498.

152.   S. Podaralla and O. Perumal, *Aaps Pharmscitech*, 2012, **13**, 919-927.

153.   B. Zhang, Y. Luo and Q. Wang, *Food Chem*. 2011, **124**, 210-220.

154.   K. Karthikeyan, V.R. Krishnaswamy, R. Lakra, M.S. Kiran and P.S. Korrapati, *Journal of Materials Science: Materials in Medicine* 2015, **26**, 101.

155.   H. Xu, L. Shen, L. Xu and Y. Yang, *Biomedical Microdevices*, 2015, **17**, 8.

156.   T. Zou and L. Gu, *Molecular pharmaceutics*, 2013, **10**, 2062-2070.

157.   L. Lai and H. Guo, *International journal of pharmaceutics*, 2011, **404**, 317-323.

158.   R. G. Aswathy, B. Sivakumar, D. Brahatheeswaran, T. Fukuda, Y. Yoshida, T. Maekawa and D. S. Kumar, *Advances in Natural Sciences: Nanoscience and Nanotechnology*, 2012, **3**, 025006.

159.   Y. Zhang, Y. Niu, Y. Luo, M. Ge, T. Yang, L. L. Yu and Q. Wang, *Food chemistry*, 2014, **142**, 269-275.

160.   S. Lee, N. S. A. Alwahab and Z. M. Moazzam, *International journal of pharmaceutics*, 2013, **454**, 388-393.

161.   J. Chen, J. Zheng, D. J. McClements and H. Xiao, *Food chemistry*, 2014, **158**, 466-472.

162.   Y. Luo, B. Zhang, M. Whent, L. L. Yu and Q. Wang, *Colloids and Surfaces B: Biointerfaces*, 2011, **85**, 145-152.

163.   Y. Luo, Z. Teng and Q. Wang, *Journal of agricultural and food chemistry*, 2012, **60**, 836-843.

164.   Y. Luo, T. T. Wang, Z. Teng, P. Chen, J. Sun and Q. Wang, *Food chemistry*, 2013, **139**, 224-230.

165.   Y. Wu, Y. Luo and Q. Wang, *LWT-Food Science and Technology*, 2012, **48**, 283-290.

166.   M. C. Regier, J. D. Taylor, T. Borcyk, Y. Yang and A. K. Pannier, *J. Nanobiotechnol*, 2012, **10**, 44.

167.   J. Gomez-Estaca, M. Balaguer, R. Gavara and P. Hernandez-Munoz, *Food Hydrocolloids*, 2012, **28**, 82-91.

168.   Y.-N. Jiang, H.-Y. Mo and D.-G. Yu, *International journal of pharmaceutics*, 2012, **438**, 232-239.

169.   W. Huang, T. Zou, S. Li, J. Jing, X. Xia and X. Liu, *AAPS PharmSciTech*, 2013, **14**, 675-681.

170.   L.-J. Sun, P.-Q. Shen and Y.-P. Zhao, *Fine Chemicals*, 2011, **3**, 014.

171.   D. Hu, C. Lin, L. Liu, S. Li and Y. Zhao, *Journal of Food Engineering*, 2012, **109**, 545-
        552.

172.   T. Zou, Z. Li, S. S. Percival, S. Bonard and L. Gu, *Food Hydrocolloids*, 2012, **27**, 293-
        300.

173.   Q. Zhong and M. Jin, *Journal of agricultural and food chemistry*, 2009, **57**, 3886-3894.

174.   I. Ezpeleta, J. M. Irache, S. Stainmesse, C. Chabenat, J. Gueguen, Y. Popineau and A.-M.
        Orecchioni, *International Journal of Pharmaceutics*, 1996, **131**, 191-200.

175.   M. A. Arangoa, M. A. Campanero, M. J. Renedo, G. Ponchel and J. M. Irache,
        Pharmaceutical research, 2001, **18**, 1521-1527.

176.   C. Duclairoir, A. Orecchioni, P. Depraetere and E. Nakache, *Journal of
        microencapsulation*, 2002, **19**, 53-60.

177.   H. Kajal and A. Misra, *Journal of biomedical nanotechnology*, 2011, **7**, 211-212.

178.   M. Gulfam, J.-e. Kim, J. M. Lee, B. Ku, B. H. Chung and B. G. Chung, *Langmuir*, 2012,
        28, 8216-8223.

179.   N. D. Young and A. K. Bharti, *Annual review of plant biology*, 2012, **63**, 283-305.

180.   Z.M. Gao, L.P. Zhu, X.Q. Yang, X.T. He, J.M. Wang, J. Guo, J.R. Qi, L.J. Wang and S.
        Yin, *Food Funct*, 2014, **5**, 1286-1293.

181.   T. Mirshahi, J. Irache, J. Gueguen and A. Orecchioni, *Drug development and industrial
        pharmacy*, 1996, **22**, 841-846.

182.   Z. Teng, Y. Luo and Q. Wang, *Journal of agricultural and food chemistry*, 2012, **60**,
        2712-2720.

183.   T. H. Wegner and E. P. Jones, *The nanoscience and technology of renewable biomaterials*, 2009, **1**, 1-41.

184.   A. Bledzki, S. Reihmane and J. Gassan, *Polym.-Plast. Technol. Eng.*, 1998, **37**, 451-468.

185.   A. Mohanty, M. Misra and L. Drzal, *Journal of Polymers and the Environment*, 2002, **10**, 19-26.

186.   L. A. Lucia and O. J. Rojas, *The nanoscience and technology of renewable biomaterials*, Wiley Online Library, 2009.

187.   D. Klemm, F. Kramer, S. Moritz, T. Lindström, M. Ankerfors, D. Gray and A. Dorris, *Angewandte Chemie International Edition*, 2011, **50**, 5438-5466.

188.   M. A. S. Azizi Samir, F. Alloin and A. Dufresne, *Biomacromolecules*, 2005, **6**, 612-626.

189.   J. F. Beecher, *Nature nanotechnology*, 2007, **2**, 466-467.

190.   J. Etang Ayuk, A. P. Mathew and K. Oksman, *Journal of Applied Polymer Science*, 2009, **114**, 2723-2730.

191.   M. J. John and S. Thomas, *Carbohydrate polymers*, 2008, **71**, 343-364.

192.   S. Kalia, A. Dufresne, B. M. Cherian, B. Kaith, L. Avérous, J. Njuguna and E. Nassiopoulos, *International Journal of Polymer Science*, 2011, **2011** doi.org/10.1155/2011/837875.

193.   A. Bledzki and J. Gassan, *Progress in polymer science*, 1999, **24**, 221-274.

194.   I. Sakurada, Y. Nukushina and T. Ito, *Journal of Polymer Science*, 1962, **57**, 651-660.

195.   H. Wei, K. Rodriguez, S. Renneckar and P.J. Vikesland, *Environ. Sci.: Nano*, 2014, **1**, 302–316.

196.   A. Dufresne, *Nanocellulose: from nature to high performance tailored materials*, Walter de Gruyter, 2012.

197.   A. Dufresne, *Materials Today*, 2013, **16**, 220-227.

198.   R. J. Moon, McGraw-Hill,Yeabook in Science & Technology, McGraw-Hill, 2008, pp. 225-228.

199.   P. Zadorecki and A. J. Michell, *Polymer Composites*, 1989, **10**, 69-77.

200.   J. Shi, S. Q. Shi, H. M. Barnes and C. U. Pittman Jr, *BioResources*, 2011, **6**, 879-890.

201.   A. Chakraborty, M. Sain and M. Kortschot, *Holzforschung*, 2005, **59**, 102-107.

202.   A. Isogai, *Journal of wood science*, 2013, **59**, 449-459.

203.   J. Zhao, W. Zhang, X. Zhang, X. Zhang, C. Lu and Y. Deng, *Carbohydrate polymers*, 2013, **97**, 695-702.

204.   E. Dinand, H. Chanzy and M. Vignon, *Cellulose*, 1996, **3**, 183-188.

205.   M. Sain and A. Bhatnagar, *CA Patent Appl*, 2003, **2**.

206.   A. Alemdar and M. Sain, *Composites Science and Technology*, 2008, **68**, 557-565.

207.   A. Dufresne, J. Y. Cavaillé and W. Helbert, *Polymer composites*, 1997, **18**, 198-210.

208.   J. Zhang, H. Song, L. Lin, J. Zhuang, C. Pang and S. Liu, *Biomass and Bioenergy*, 2012, **39**, 78-83.

209.   A. Dufresne, D. Dupeyre and M. R. Vignon, *Journal of Applied Polymer Science*, 2000, **76**, 2080-2092.

210.   X. Cao, Y. Chen, P. R. Chang, M. Stumborg and M. A. Huneault, *Journal of Applied Polymer Science*, 2008, **109**, 3804-3810.

211.   B. Wang, M. Sain and K. Oksman, *Applied Composite Materials*, 2007, **14**, 89-103.

212.   B. Wang and M. Sain, *Polymer International*, 2007, **56**, 538-546.

213.   E. Dinand, H. Chanzy and R. Vignon, *Food Hydrocolloids*, 1999, **13**, 275-283.

214.   A. Dufresne, J.-Y. Cavaille and M. R. Vignon, *Journal of applied polymer science*, 1997, **64**, 1185-1194.

215.   C. Goussé, H. Chanzy, M. Cerrada and E. Fleury, *Polymer*, 2004, **45**, 1569-1575.

216.   Y. Habibi and M. R. Vignon, *Cellulose*, 2008, **15**, 177-185.

217.   D. Bhattacharya, L. T. Germinario and W. T. Winter, *Carbohydrate Polymers*, 2008, **73**, 371-377.

218.   E. d. M. Teixeira, D. Pasquini, A. A. Curvelo, E. Corradini, M. N. Belgacem and A. Dufresne, *Carbohydrate Polymers*, 2009, **78**, 422-431.

219.   J. Li, X. Wei, Q. Wang, J. Chen, G. Chang, L. Kong, J. Su and Y. Liu, *Carbohydrate polymers*, 2012, **90**, 1609-1613.

220.   Y. Lu, L. Weng and X. Cao, *Macromolecular Bioscience*, 2005, **5**, 1101-1107.

221.   X. Cao, Y. Chen, P. Chang, A. Muir and G. Falk, *Express Polym Lett*, 2008, **2**, 502-510.

222.   Y. Lu, L. Weng and X. Cao, *Carbohydrate polymers*, 2006, **63**, 198-204.

223.   Y. Chen, C. Liu, P. R. Chang, D. P. Anderson and M. A. Huneault, *Polymer Engineering & Science*, 2009, **49**, 369-378.

224.   Y. Chen, C. Liu, P. R. Chang, X. Cao and D. P. Anderson, *Carbohydrate Polymers*, 2009, **76**, 607-615.

225.   M. Jonoobi, J. Harun, P. M. Tahir, A. Shakeri, S. SaifulAzry and M. D. Makinejad, *Materials Letters*, 2011, **65**, 1098-1100.

226.   M. Jonoobi, K. O. Niska, J. Harun and M. Misra, *BioResources*, 2009, **4**, 626-639.

227.   M. Joonobi, J. Harun, P. M. Tahir, L. H. Zaini, S. SaifulAzry and M. D. Makinejad, *BioResources*, 2010, **5**, 2556-2566.

228.   H. Kargarzadeh, I. Ahmad, I. Abdullah, A. Dufresne, S. Y. Zainudin and R. M. Sheltami, *Cellulose*, 2012, **19**, 855-866.

229.   L. H. Zaini, M. Jonoobi, P. M. Tahir and S. Karimi, 2013. *J. Biomater. Nanobiotech*, 2013, **4,** DOI:10.4236/jbnb.2013.41006.

230.   A. Alemdar and M. Sain, *Bioresource technology*, 2008, **99**, 1664-1671.

231.   M. Jonoobi, A. Khazaeian, P. M. Tahir, S. S. Azry and K. Oksman, *Cellulose*, 2011, **18**, 1085-1095.

232.   N. Ngadi and N. S. Lani, *Jurnal Teknologi*, 2014, **68**.

233.   D. Bruce, R. Hobson, J. Farrent and D. Hepworth, *Composites Part A: Applied Science and Manufacturing*, 2005, **36**, 1486-1493.

234.   J. I. Morán, V. A. Alvarez, V. P. Cyras and A. Vázquez, *Cellulose*, 2008, **15**, 149-159.

235.   X. Cao, B. Ding, J. Yu and S. S. Al-Deyab, *Carbohydrate polymers*, 2012, **90**, 1075-1080.

236.   M. S. Jahan, A. Saeed, Z. He and Y. Ni, *Cellulose*, 2011, **18**, 451-459.

237.   R. Zuluaga, J.-L. Putaux, A. Restrepo, I. Mondragon and P. Ganán, *Cellulose*, 2007, **14**, 585-592.

238.   N. Johar, I. Ahmad and A. Dufresne, *Industrial Crops and Products*, 2012, **37**, 93-99.

239.   L. Ludueña, D. Fasce, V. A. Alvarez and P. M. Stefani, *BioResources*, 2011, **6**, 1440-1453.

240.   F. Fahma, S. Iwamoto, N. Hori, T. Iwata and A. Takemura, *Cellulose*, 2011, **18**, 443-450.

241.   M. Rosa, E. Medeiros, J. Malmonge, K. Gregorski, D. Wood, L. Mattoso, G. Glenn, W. Orts and S. Imam, *Carbohydrate Polymers*, 2010, **81**, 83-92.

242.   R. M. Sheltami, I. Abdullah, I. Ahmad, A. Dufresne and H. Kargarzadeh, *Carbohydrate Polymers*, 2012, **88**, 772-779.

243.   H. El-Saied, A. H. Basta and R. H. Gobran, *Polymer-Plastics Technology and Engineering*, 2004, **43**, 797-820.

244.   E. E. Brown and M.-P. G. Laborie, *Biomacromolecules*, 2007, **8**, 3074-3081.

245.   M. Iguchi, S. Yamanaka and A. Budhiono, *Journal of Materials Science*, 2000, **35**, 261-270.

246.   Y. Dahman, *Journal of nanoscience and nanotechnology*, 2009, **9**, 5105-5122.

247.   C. J. Grande, F. G. Torres, C. M. Gomez, O. P. Troncoso, J. Canet-Ferrer and J. Martinez-Pastor, *Polymers & polymer composites*, 2008, **16**, 181-185.

248.   S. Ifuku, M. Nogi, K. Abe, K. Handa, F. Nakatsubo and H. Yano, *Biomacromolecules*, 2007, **8**, 1973-1978.

249.   H. Maeda, M. Nakajima, T. Hagiwara, T. Sawaguchi and S. Yano, *Journal of materials science*, 2006, **41**, 5646-5656.

250.   A. Nakagaito, S. Iwamoto and H. Yano, *Applied Physics A*, 2005, **80**, 93-97.

251.   M. Nogi, S. Ifuku, K. Abe, K. Handa, A. N. Nakagaito and H. Yano, *Applied Physics Letters*, 2006, **88**, Thesis no. 133124, doi: 10.1063/1.2191667.

252.   M. Nogi and H. Yano, *Advanced Materials*, 2008, **20**, 1849-1852.

253.   H. Yano, J. Sugiyama, A. N. Nakagaito, M. Nogi, T. Matsuura, M. Hikita and K. Handa, *Advanced Materials*, 2005, **17**, 153-155.

254.   S. Yano, H. Maeda, M. Nakajima, T. Hagiwara and T. Sawaguchi, *Cellulose*, 2008, **15**, 111-120.

255.   M. A. Hubbe, O. J. Rojas, L. A. Lucia and M. Sain, *BioResources*, 2008, **3**, 929-980.

256.   A. Nakagaito and H. Yano, *Applied Physics A*, 2004, **78**, 547-552.

257.   S. Iwamoto, A. Nakagaito, H. Yano and M. Nogi, *Applied Physics A*, 2005, **81**, 1109-1112.

258.   M. E. Malainine, M. Mahrouz and A. Dufresne, *Composites Science and Technology*, 2005, **65**, 1520-1526.

259.   M. Andresen, L.-S. Johansson, B. S. Tanem and P. Stenius, *Cellulose*, 2006, **13**, 665-677.

260.   M. Andresen and P. Stenius, *Journal of dispersion science and technology*, 2007, **28**, 837-844.

261.   P. Stenstad, M. Andresen, B. S. Tanem and P. Stenius, *Cellulose*, 2008, **15**, 35-45.

262.   K. Syverud and P. Stenius, *Cellulose*, 2009, **16**, 75-85.

263.   A. Bhatnagar and M. Sain, *Journal of Reinforced Plastics and Composites*, 2005, **24**, 1259-1268.

264.   B. Wang and M. Sain, *Composites Science and Technology*, 2007, **67**, 2521-2527.

265.   K. L. Spence, R. A. Venditti, O. J. Rojas, Y. Habibi and J. J. Pawlak, *Cellulose*, 2011, **18**, 1097-1111.

266.   K. Abe, S. Iwamoto and H. Yano, *Biomacromolecules*, 2007, **8**, 3276-3278.

267.   S. Iwamoto, A. Nakagaito and H. Yano, *Applied Physics A*, 2007, **89**, 461-466.

268.   M. Henriksson, L. A. Berglund, P. Isaksson, T. Lindstrom and T. Nishino, *Biomacromolecules*, 2008, **9**, 1579-1585.

269.   S. Karimi, A. Dufresne, P. M. Tahir, A. Karimi and A. Abdulkhani, *Journal of Materials Science*, 2014, **49**, 4513-4521.

270.   B. Wang and M. Sain, *Bioresources*, 2007, **2**, 371-388.

271.   E. Lasseuguette, D. Roux and Y. Nishiyama, *Cellulose*, 2008, **15**, 425-433.

272. T. Saito, M. Hirota, N. Tamura, S. Kimura, H. Fukuzumi, L. Heux and A. Isogai, *Biomacromolecules*, 2009, **10**, 1992-1996.

273. T. Saito and A. Isogai, *Carbohydrate Polymers*, 2005, **61**, 183-190.

274. T. Saito and A. Isogai, *Colloids and Surfaces A: Physicochemical and Engineering Aspects*, 2006, **289**, 219-225.

275. T. Saito and A. Isogai, *Industrial & engineering chemistry research*, 2007, **46**, 773-780.

276. T. Saito, S. Kimura, Y. Nishiyama and A. Isogai, *Biomacromolecules*, 2007, **8**, 2485-2491.

277. T. Saito, Y. Nishiyama, J.-L. Putaux, M. Vignon and A. Isogai, *Biomacromolecules*, 2006, **7**, 1687-1691.

278. A. Isogai, T. Saito and H. Fukuzumi, *Nanoscale*, 2011, **3**, 71-85.

279. F. Jiang and Y.-L. Hsieh, *Carbohydrate polymers*, 2013, **95**, 32-40.

280. M. Henriksson, G. Henriksson, L. Berglund and T. Lindström, *European Polymer Journal*, 2007, **43**, 3434-3441.

281. M. Pääkkö, M. Ankerfors, H. Kosonen, A. Nykänen, S. Ahola, M. Österberg, J. Ruokolainen, J. Laine, μ. T. Larsson and O. Ikkala, *Biomacromolecules*, 2007, **8**, 1934-1941.

282. S. Janardhnan and M. M. Sain, *Bioresources*, 2007, **1**, 176-188.

283. I. Siró and D. Plackett, *Cellulose*, 2010, **17**, 459-494.

284. M. M. de Souza Lima and R. Borsali, *Macromolecular Rapid Communications*, 2004, **25**, 771-787.

285. I. M. Saxena and R. M. Brown, *Annals of botany*, 2005, **96**, 9-21.

286. W. Thielemans, C. R. Warbey and D. A. Walsh, *Green Chemistry*, 2009, **11**, 531-537.

287. S. Camarero Espinosa, T. Kuhnt, E. J. Foster and C. Weder, *Biomacromolecules*, 2013, **14**, 1223-1230.

288. M. N. Angles and A. Dufresne, *Macromolecules*, 2000, **33**, 8344-8353.

289. A. P. Mathew and A. Dufresne, *Biomacromolecules*, 2002, **3**, 1101-1108.

290. A. P. Mathew, W. Thielemans and A. Dufresne, *Journal of Applied Polymer Science*, 2008, **109**, 4065-4074.

291. A. J. Carvalho, *Starch: major sources, properties and applications as thermoplastic materials*, Elsevier, Amsterdam, 2008.

292. P.M. Visakh, P.M. Aji, K. Oksman and S. Thomas, Starch-Based Bionanocomposites: Processing and Properties, Editors: Y. Habibi, L.A. Lucia, *Polysaccharide Building Blocks: A Sustainable Approach to the Development of Renewable Biomaterials*, 2012, 287-306, John Wiley and Sons.

293. H. Zobel, *Starch‑Stärke*, 1988, **40**, 44-50.

294. A. Imberty, A. Buléon, V. Tran and S. Péerez, *Starch‑Stärke*, 1991, **43**, 375-384.

295. F. Xie, E. Pollet, P. J. Halley and L. Avérous, *Progress in Polymer Science*, 2013, **38**, 1590-1628.

296. H. Liu, L. Yu, F. Xie and L. Chen, *Carbohydrate Polymers*, 2006, **65**, 357-363.

297. F. Xie, L. Yu, B. Su, P. Liu, J. Wang, H. Liu and L. Chen, *Journal of Cereal Science*, 2009, **49**, 371-377.

298. D. Le Corre, J. Bras and A. Dufresne, *Biomacromolecules*, 2010, **11**, 1139-1153.

299. A. Dufresne, J.-Y. Cavaille and W. Helbert, *Macromolecules*, 1996, **29**, 7624-7626.

300. J.-L. Putaux, S. Molina-Boisseau, T. Momaur and A. Dufresne, *Biomacromolecules*, 2003, **4**, 1198-1202.

301. G. Chen, M. Wei, J. Chen, J. Huang, A. Dufresne and P. R. Chang, *Polymer*, 2008, **49**, 1860-1870.

302. Y. Chen, X. Cao, P. R. Chang and M. A. Huneault, *Carbohydrate Polymers*, 2008, **73**, 8-17.

303. H. Zheng, F. Ai, P. R. Chang, J. Huang and A. Dufresne, *Polymer Composites*, 2009, **30**, 474-480.

304. N. L. García, L. Ribba, A. Dufresne, M. I. Aranguren and S. Goyanes, *Macromolecular Materials and Engineering*, 2009, **294**, 169-177.

305. H. Namazi and A. Dadkhah, *Journal of applied polymer science*, 2008, **110**, 2405-2412.

306. H. Angellier, S. Molina-Boisseau and A. Dufresne, *Macromolecules*, 2005, **38**, 9161-9170.

307. F. Fathi, A. Dadkhah and H. Namazi, *International Journal of Nanoparticles*, 2014, **7**, 37-48.

308. Y. Wang and L. Zhang, *Journal of nanoscience and nanotechnology*, 2008, **8**, 5831-5838.

309. Y. Xu, E. N. Sismour, C. Grizzard, M. Thomas, D. Pestov, Z. Huba, T. Wang and H. L. Bhardwaj, *Cereal Chemistry*, 2014, **91**, 383-388.

310. H. Angellier, L. Choisnard, S. Molina-Boisseau, P. Ozil and A. Dufresne, *Biomacromolecules*, 2004, **5**, 1545-1551.

311. N. Lin and A. Dufresne, Nanoscale, 2014, 6, 5384-5393

312. M. Kaushik, K. Basu, C. Benoit, C.M. Cirtiu, H. Vali and A. Moores, *J. Am. Chem. Soc*, 2015, **137**, 6124–6127.

313.   J. Qu, C. Luo, Q. Zhang, Q. Cong and X. Yuan, *Materials Science and Engineering: B*, 2013, **178**, 380–382.

314.   J. Qu, Q. Zhang, Y. Xia, Q. Cong and C. Luo, *Environ Sci Pollut Res Int*, 2015, **22**, 1408-1419.

315.   P. Roy, A.P. Periasamy, C. Chuang, Y.-R Liou, Y.-F Chen, J. Joly, C.-Te Liang and H.-T. Chang, *New J. Chem*, 2014, **38**, 4946-4951.

316.   I. Rhee, Y.A. Kim, G.-O Shin, J.H. Kim and H. Muramatsu, *Construction and Building Materials*, 2015, **96**, 189–197.

317.   C. Wang, D. Ma and X. Bao, *The Journal of Physical Chemistry C*, 2008, **112**, 17596-17602.

318.   M. Saxena and S. Sarkar, *Materials Express*, 2013, **3**, 201-209.

319.   M. Ghosh, S. K. Sonkar, M. Saxena and S. Sarkar, *Small*, 2011, **7**, 3170-3177.

320.   S. K. Sonkar, M. Ghosh, M. Roy, A. Begum and S. Sarkar, *Materials Express*, 2012, **2**, 105-114.

321.   S. KumaráSonkar and D. GorakháBabar, *Nanoscale*, 2012, **4**, 7670-7675.

322.   C. Journet, M. Picher and V. Jourdain, *Nanotechnology*, 2012, **23**, 142001.

323.   M. F. De Volder, S. H. Tawfick, R. H. Baughman and A. J. Hart, *Science*, 2013, **339**, 535-539.

324.   B. Goodell, X. Xie, Y. Qian, G. Daniel, M. Peterson and J. Jellison, *Journal of nanoscience and nanotechnology*, 2008, **8**, 2472-2474.

325.   S. Paul, 2013, Thesis, http://ir.inflibnet.ac.in:8080/jspui/handle/10603/9008.

326.   X. Ye, Q. Yang, Y. Zheng, W. Mo, J. Hu and W. Huang, *Materials Research Bulletin*, 2014, **51**, 366-371.

327.   X. Xie, B. Goodell, Y. Qian, G. Daniel, D. Zhang, D. C. Nagle, M. L. Peterson and J. Jellison, *Forest products journal*, 2009, **59**, 26-28.

328.   J. Zhao, X. Guo, Q. Guo, L. Gu, Y. Guo and F. Feng, *Carbon*, 2011, **49**, 2155-2158.

329.   L. Dubrovina, O. Naboka, V. Ogenko, P. Gatenholm and P. Enoksson, *Journal of Materials Science*, 2014, **49**, 1144-1149.

330.   H. Li, Z. Kang, Y. Liu and S.-T. Lee, *Journal of materials chemistry*, 2012, **22**, 24230-24253.

331.   P.-C. Hsu, Z.-Y. Shih, C.-H. Lee and H.-T. Chang, *Green Chemistry*, 2012, **14**, 917-920.

332.   B. De and N. Karak, *Rsc Advances*, 2013, **3**, 8286-8290.

333.   Shi L, Li X, Li Y, Wen X, Li J, Choi MMF, Dong C and S. Shuang, *Sensors and Actuators B: Chemical*, 2015, **210**, 533-541.

334.   S. Sahu, B. Behera, T. K. Maiti and S. Mohapatra, *Chemical Communications*, 2012, **48**, 8835-8837.

335.   S. Gao, Y. Chen, H. Fan, X. Wei, C. Hu, L. Wang and L. Qu, *Journal of Materials Chemistry A*, 2014, **2**, 6320-6325.

336.   W. Lu, X. Qin, S. Liu, G. Chang, Y. Zhang, Y. Luo, A. M. Asiri, A. O. Al-Youbi and X. Sun, *Analytical chemistry*, 2012, **84**, 5351-5357.

337.   Yu J, Song N, Zhang Y-K, Zhong S-X, Wang A-J and J. Chen, *Sensors and Actuators B: Chemical*, 2015, **214**, 29-35.

338.   A. Mewada, S. Pandey, S. Shinde, N. Mishra, G. Oza, M. Thakur, M. Sharon and M. Sharon, *Materials Science and Engineering: C*, 2013, **33**, 2914-2917.

339.   Y. Liu, Y. Zhao and Y. Zhang, *Sensors and Actuators B: Chemical*, 2014, **196**, 647-652.

340.   J. Xu, Y. Zhou, S. Liu, M. Dong and C. Huang, *Analytical Methods*, 2014, **6**, 2086-2090.

341. A. Prasannan and T. Imae, *Industrial & Engineering Chemistry Research*, 2013, **52**, 15673-15678.

342. S. Y. Park, H. U. Lee, E. S. Park, S. C. Lee, J.-W. Lee, S. W. Jeong, C. H. Kim, Y.-C. Lee, Y. S. Huh and J. Lee, *ACS applied materials & interfaces*, 2014, **6**, 3365-3370.

343. M. Zhang, M. Liu, S. Bewick and Z. Suo, *Journal of biomedical nanotechnology*, 2009, **5**, 294-299.

344. S. C. Lenaghan and M. Zhang, *Plant Science*, 2012, **183**, 206-211.

345. M. Zhang, S. C. Lenaghan, L. Xia, L. Dong, W. He, W. R. Henson and X. Fan, Journal of nanobiotechnology, 2010, 8, 20.

346. S. C. Lenaghan, L. Xia and M. Zhang, *Journal of biomedical nanotechnology*, 2009, **5**, 472-476.

347. K. H. N. Liu, M. T. McDowell, J. Zhao and Y. Cui, Scientific Reports, 2013, **3**, 1919. .

348. W. Wang, J. C. Martin, X. Fan, A. Han, Z. Luo and L. Sun, *ACS applied materials & interfaces*, 2012, **4**, 977-981.

349. H. Chen, W. Wang, J. C. Martin, A. J. Oliphant, P. A. Doerr, J. F. Xu, K. M. DeBorn, C. Chen and L. Sun, *ACS Sustainable Chemistry & Engineering*, 2012, **1**, 254-259.

350. A. Xing, S. Tian, H. Tang, D. Losic and Z. Bao, *RSC Advances*, 2013, **3**, 10145-10149.

351. M. Salavati-Niasari, J. Javidi and M. Dadkhah, *Combinatorial chemistry & high throughput screening*, 2013, **16**, 458-462.

352. S. C. L. J. N. Burris, M. Zhang and C. N. Stewart, *Journal of Nanobiotechnology*, 2012, **10**, 41.

353. A. M. R. J. Moon, J. Nairn, J. Simonsenf and J. Youngblood, *Chem. Soc. Rev*, 2011, **40**, 3941-3994.

354.   Y. Wang and A. Hu. *J. Mater. Chem. C*, 2014,**2**, 6921-6939..

355.   R. J. W. M-M. Titirici, N. Brun, V. L. Budarin, D. S. Su, F. del Monte, J. H. Clarkd and

M. J. MacLachlang, *Chem. Soc. Rev.*, 2015, **44**, 250-290.

356.   Q. W. Y. Luo, *J. Appl. Polym. Sci.* 2014, doi: 10.1002/APP.40696.